# RADAR to RADAR Interference
# for 77GHz Automotive RADARs

Thesis submitted in partial fulfillment of the degree of
## Master of Science
in
## Electrical Engineering
(Microelectronics)

By

## Sasanka  Sanka
4519558

23rd November 2017

**T**U Delft
Delft
University of
Technology

Electronic Research Laboratory
Electrical Engineering, Mathematics and Computer Science
Delft University of Technology
The Netherlands

In cooperation with





Prof. Dr. Alexander  Yarovoy
Asst. Prof. Dr. Faruk Uysal
Assoc. Prof. Dr.ir. Gerard  J.M. Janssen

Feike Jansen

# Delft University of Technology
## Faculty of Electrical Engineering, Mathematics and Computer Science

The under-signed hereby certify that the thesis titled **RADAR to RADAR Interference for 77GHz Automotive RADARs** by **Sasanka   Sanka** fulfills the requirements for the degree of **Master of Science,** and recommend to the Faculty of Electrical Engineering, Mathematics and Computer Science for the acceptance of the thesis.

**Date:**  November 23rd, 2017

**Chairman**

—————————————————

Prof. dr. Alexander Yarovoy
MS3, TU Delft

**Committee Members**

—————————————————

Dr. Faruk Uysal
MS3, TU Delft

—————————————————

Dr.ir. Gerard J.M.Janssen
CAS, TU Delft

—————————————————

Feike Jansen
NXP Semiconductors

*Don't find fault, find a remedy.*

Henry Ford

# CONTENTS

# PREFACE

# ABSTRACT

Automotive radar is a key element in Advanced Driver Assistance Systems (ADAS). With the growth of Automotive industry, there is a high demand for the sensors used in assisting systems. As the number of sensors increases, probability that these systems being in close proximity will also increase. This will lead to situations where in multiple radar sensors will be operating in close proximity, this might lead to a sub-optimal performance of our radar system. Currently FMCW radar systems are most prevalent in the automotive radar market. For FMCW systems, interference mitigation techniques exist in time domain, frequency domain, polarization domain and etc. Most of these techniques insist on detecting and identifying the interference before mitigating it.

In this thesis, we consider a FMCW radar system and first develop a MATLAB model for the three most important interference scenarios namely Continuous Wave(CW), Frequency Modulated Continuous Wave(FMCW) and Phase Modulated Continuous Wave(PMCW). We propose a signal model where interference can be localized over the beat signal, then we systematically study how interference can be detected. As a result, we will detect the interference even if the power level of the interferer is lower than the power level of the received reflected signal.

Post detection of interference, we suggest a technique to identify the interference by estimating the slope from the detected interference samples. Starting with a simple existing mitigation technique, we look at how to mitigate the interference and suggest enhancements that can be done for these techniques post detection and identification. Considering a worst case scenario of interference being completely in band to the transmitted signal, we propose a novel avoidance technique which will also predict the bandwidth of the interferer. As a result we will be able to shift the center frequency of the transmitter to avoid the interferer.

Finally we propose another novel time domain mitigation technique where in without detecting or identifying the interferer, we will mitigate the interference and compare the gain of Signal to Interference plus Noise Ratio (SINR) achieved by using this technique.

# 1

# INTRODUCTION

In a world taken over by technology, consumer products which use to have physical significance are being connected to technology to make them more reliable. In the advent of communications, it is also necessary that these products communicate with each other to reduce the probability of interfering. Imagine a situation where two autonomous vehicles sensors interfering with each other and limiting their performance. It is obvious that in future this situation might occur with growing autonomous vehicle industry. This is why there is a need for a reliable and robust technology for these vehicular sensors.

Currently, automobiles use a multitude of sensor technologies to make themselves more reliable. Especially to assist drivers, Advanced Driver-Assistance Systems (ADAS) are developed to automate/adapt/enhance vehicle systems for safety and better driving. ADAS relies on input from all the available sensors based on optical, LiDAR and RADAR.

Radars are extensively used in automobiles as they work in any atmospheric condition and are very reliable. Most of the existing radars use pulse based systems, where a single pulse is transmitted and received. Radars using frequency modulation are very prevalent in industry. Phase modulation also has accrued a lot of interest in the recent times. FMCW is preferred over pulse based radars in automotive because it requires less peak power for transmission when compared to the pulsed based radar and also pulsed radars cannot receive and transmit simultaneously.

## 1.1. MOTIVATION

Automotive radar systems will become more and more prevalent in the near future. This will lead to a situation where multiple radars will be operating in a close proximity and in the same frequency band. It was proved that radars operating closely will have deleterious effects on the performance of each other [1],[2],[3]. Hence there is a need to study mutual interference between these radar sensors. A detailed description on FMCW radar in the presence of interference and also a description of gain versus deterministic interference is given in [4].

**1**

In order to tackle this problem of interference from other radars, first we have to detect the presence of interferer. Post detection, the interference has to be mitigated.

## 1.2. RESEARCH GOAL

This thesis will be aimed at a detailed study of interference effects in FMCW radars. In order to mitigate interference, first we should be able to detect it. Most of the existing techniques detect and mitigate the interference only if the interference power is much higher than the received reflected signal power.

First goal of our research is to understand the effect of interference peak power on the received signal. Consequently, to find if there is a way to detect the interference even if the interferer power level is lower than the received reflected signal power and to find ways to localize the interference.

With this information on detection, the next goal is to explore if there is anything that we can learn about the parameters of the interferer itself such as the slope and the type of the interferer.

Finally, we would like to investigate mitigation and avoidance strategies for the interferer even when the interferer power is lower than the received reflected signal power.

## 1.3. NOVELTY

This thesis was aimed at giving a very detailed study on interference in FMCW radars. The main goal was to study the detection, localization, identification, avoidance and mitigation of interference in FMCW radars.

The novel aspect in this thesis can be summarized as follows

1. Proved the existence of interference in wider bands while processing even if the interference is short.

2. A method for detecting the interference even when the power level of the interferer is lower than the power level of the received reflected signal.

3. A method to identify the slope of the interferer through the detected interference signal.

4. A one-shot interference avoidance technique by estimating the frequency shift.

5. A method to mitigate interference blindly by using compressive sensing techniques.

## 1.4. THESIS OUTLINE

In Chapter 1, we look at the basics of radar including FMCW and PMCW waveforms and their generation. We first look at the existing state of the art mitigation techniques and different domains in which mitigation can be done in Chapter 2. In Chapter 3 we study how the interference would look like in FMCW radar system. We explain in detail why interference might affect our FMCW system, we systematically study how interference looks in the time domain, frequency domain and angular domain with necessary equations. In Chapter 4, we propose a way to detect interfering samples with the help of a

High Pass Filter(HPF) and Constant False Alarm Rate (CFAR) thresholding. Chapter 5 describes a method for identifying the interferer by estimating the slope from detected interference samples and also propose a strategic detect and avoid technique by using slope estimation. In Chapter 6, with the comparison of existing mitigation techniques in the industry, we propose a novel time domain mitigation technique by using compressed sensing techniques.

The proposed processing chain for mitigation and avoidance of interference is shown in Fig 1.1. Avoidance chain starts with detecting the interference by using a High Pass Filter(HPF) and a Constant False Alarm Rate(CFAR) detector. Post detection, we describe our identification algorithm. From the information obtained through the identification algorithm, a strategic detect and avoid technique will be used to avoid interference.

In the mitigation chain, the received decimated signal is looked at the transforms for which the interference and beat signal are sparse. We apply a dual basis pursuit algorithm which separates the interference from the beat signal. With the obtained coefficients for beat signal, we apply the inverse transform for the sparse beat signal coefficients to get the interference mitigated beat signal.

1
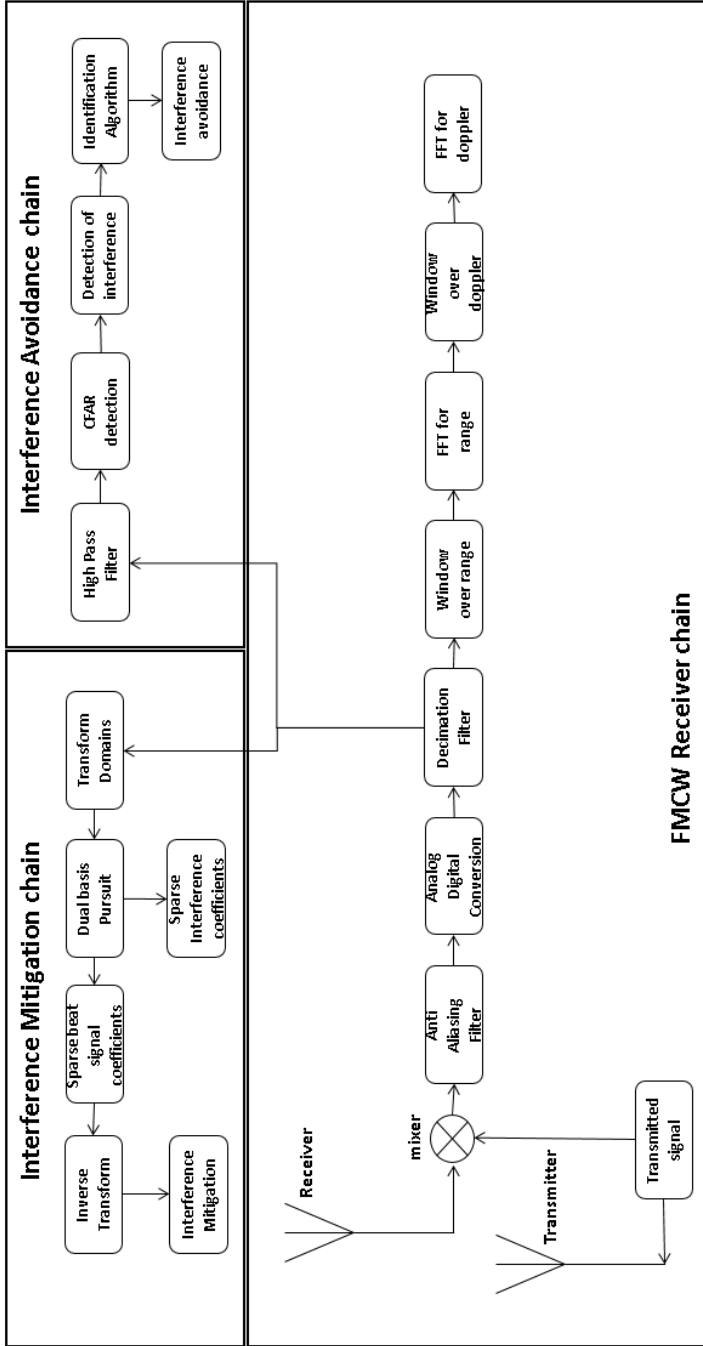


Figure 1.1: Interference chain implemented

## 1.5. FUNDAMENTALS OF RADAR

RAdio Detection And Ranging (RADAR) describes the very general principle of using electro-magnetic waves to detect and possibly locate objects. When an Electro-Magnetic (EM) wave is transmitted, the received response of transmitted EM wave is compared with the transmitted wave and the information regarding range and velocity of the object can be estimated. When an EM pulse is transmitted into a medium, due to discontinuities(objects) present in the medium, a fraction of EM pulse is reflected back. A monostatic radar in which receiver and transmitter are collocated is considered for detailed explanation in this section. From the point of transmission to the point of reception, the EM wave travels $2R$ in distance and $\tau$ in time. $R$ is the range of object with respect to the radar, and can be estimated as

$$R = c\tau/2, \tag{1.1}$$

where, $c$ is the speed of light, Equation (1.1) is the basic range equation for any radar application and is only true if the transmitter and receiver are not moving relatively to each other. If there is a relative motion between the radar transmitter and the object, we would observe a Doppler effect and it is given as

$$f_d = f_c(2v/c). \tag{1.2}$$

Here $f_d$ is the Doppler frequency shift, $v$ is the relative velocity between the transmitter and receiver and $f_c$ is the center frequency of transmitted signal.

## 1.6. FMCW SYSTEM INTRODUCTION

FMCW consists of a chirp signal or Linear Frequency Modulated (LFM) signal which is transmitted at a certain carrier frequency. This transmitted signal is received after a time delay which is proportional to the range of the object, on the other hand velocity estimation is dependent on the difference in phase between the transmitted and received signal. Since FMCW is a continuous wave phenomenon, the received signal is compared with the transmitted signal to obtain the information on the range and Doppler processing is applied to obtain velocity information of the object. The typical FMCW equations for a single ramp in [5] are re-visited here. The instantaneous transmission frequency of the ramp $f_t$ having a bandwidth from $(0, B)$ is,

$$f_t = \frac{B}{T}t \qquad 0 < t < T. \tag{1.3}$$

where, $T$ is the time period of the ramp, $t$ is time extending from $(0, T)$ for a single ramp. The received frequency can be described as a time delayed version of the transmitted frequency given as,

$$f_r = \frac{B}{T}(t - \tau_1) \qquad 0 < t < T \tag{1.4}$$

Where $f_r$ is the received instantaneous frequency, $\tau_1$ is the time delay given by, $\tau_1 = 2(R + vt)/c$, $v$ is relative radial velocity of the object and $R$ as the initial range of object. A single chirp transmission and reception with a delay of $10\mu s$ is shown in Fig 1.2

**1**
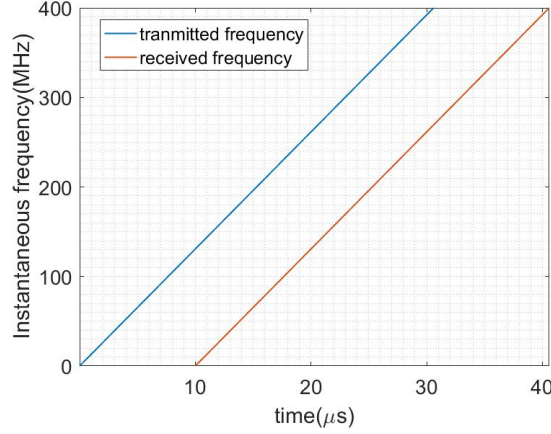


Figure 1.2: Instantaneous Frequency for transmission and reception

For better understanding of our problem and to infer some results, we make use of a rectangular function. A typical rectangular function can be defined as a function that is 0 outside the interval [-T/2,T/2] and unity inside it, where T is the time period of our signal. A rectangular function is described as

$$\text{Rect}\left(\frac{t}{T}\right) = 1 \quad -T/2 \le t \le T/2 \tag{1.5}$$

An extended version of this function with a delay $\tau$ is given as follows

$$\text{Rect}\left(\frac{t - T/2 - \tau}{T}\right) = \begin{cases} 1 & \tau \le t \le T + \tau \\ 0 & otherwise \end{cases} \tag{1.6}$$

hence the transmitted FMCW signal for a single ramp is given as,

$$s_t = \text{Rect}\left(\frac{t - T/2}{T}\right) \exp\left(2j\pi\left(f_c t + \int_t^{T+t} f_t \partial t\right)\right)$$

$$s_t = \text{Rect}\left(\frac{t - T/2}{T}\right) \exp\left(2j\pi\left(f_c t + \frac{B}{2T} t^2\right)\right) \tag{1.7}$$

where, $f_c$ is the carrier frequency of the transmitted signal. There are some benefits of using a complex signal in understanding the interference which will be shown in the further chapters. In reality, we only transmit the real part of the signal $s_t$. The received signal is time shifted by $\tau_1$ from the transmitted signal is given by ,

$$s_r = \text{Rect}\left(\frac{t - T/2 - \tau_1}{T}\right) \exp\left(2j\pi\left(f_c(t - \tau_1) + \frac{B}{2T}(t - \tau_1)^2\right)\right) \tag{1.8}$$

For this thesis, we have used the chirp time as $30.6\mu s$ and an acquisition time of $25.6\mu s$. The first $5\mu s$ of $30.6\mu s$ is to make sure the Phase Locked Loop(PLL) achieves linearity,

this interval will be neglected while processing. This gives us an effective acquisition time of $25.6\mu s$. The received signal is mixed with the transmitted signal to obtain the information of range and velocity. The mixer signal is given as $s_m$,

$$s_m = s_r s_t^*$$

$$s_m = \text{Rect}\left(\frac{t - T/2 - \tau_1}{T - \tau_1}\right)\exp\left(-2j\pi\left(f_c\,\tau_1 - \frac{B}{2T}(\tau_1)^2 + \frac{B}{T}t\,\tau_1\right)\right) \tag{1.9}$$

Multiplication of a rectangular function with a time shifted version of itself will result in a rectangular function of shorter time span. Hence the two rectangular functions, in transmission of span $T$ and reception of span $T$ but with a delay of $\tau_1$ will result in a rectangular function of a shorter time span of $T - \tau_1$, the use of this notational is very important for us as we see in the following chapters that the interference can be represented as a time limited function using rectangular functions.

Since, the generation and transmission of data at 77 GHz would require sampling at a frequency higher than 154 GHz, we consider an equivalent baseband simulation model for transmission and reception. The effect of center frequency of the interferer will also be studied in later sections. But for all the simulations, we have considered a worst case scenario that both the transmitted and interferer signal are having same center frequency. Also for better understanding of the interference, we have considered complex signals for simulations. But it is to be understood that all these signals generated should be real valued. For real valued transmit signals a simple receive equations in presence of In-phase and Quadrature channels will give a complex signal as output is given as follows,

$$s_t = \text{Rect}\left(\frac{t - T/2}{T}\right)\text{Cos}\left(2\pi\left(f_c t + \frac{B}{2T}t^2\right)\right) \tag{1.10}$$

and the received signal as

$$s_r = \text{Rect}\left(\frac{t - T/2 - \tau_1}{T}\right)\text{Cos}\left(2\pi\left(f_c(t - \tau_1) + \frac{B}{2T}(t - \tau_1)^2\right)\right) \tag{1.11}$$

Now the I/Q demodulator consists of two mixers to generate In-phase(I) and Quadrature(Q) components by multiplying the received signal $s_r$ with $\text{Sin}(\phi_t)$ and $\text{Cos}(\phi_t)$ respectively to give

$$I(t) = \text{Rect}\left(\frac{t - T/2 - \tau_1}{T}\right)\frac{1}{2}\left(\text{Cos}\left(\phi_r - \phi_t\right) + \text{Cos}\left(\phi_r + \phi_t\right)\right) \tag{1.12}$$

$$Q(t) = \text{Rect}\left(\frac{t - T/2 - \tau_1}{T}\right)\frac{1}{2}\left(\text{Sin}\left(\phi_r - \phi_t\right) + \text{Sin}\left(\phi_r + \phi_t\right)\right) \tag{1.13}$$

where, $\phi_t = \left(2\pi\left(f_c t + \frac{B}{2T}t^2\right)\right)$ and $\phi_r = \left(2\pi\left(f_c(t - \tau_1) + \frac{B}{2T}(t - \tau_1)^2\right)\right)$.

The higher frequency components $(\phi_t + \phi_r)$ are filtered out by the Anti-Aliasing filter and hence the residual In-phase component is given as

$$I(t) = \text{Rect}\left(\frac{t - T/2 - \tau_1}{T}\right)\left(\frac{1}{2}\text{Cos}\left(2\pi\left(-f_c\tau_1 + \frac{B}{2T}\tau_1^2 - \frac{B}{T}\tau_1 t\right)\right)\right) \tag{1.14}$$

similarly Quadrature component can also be calculated. Substituting $\tau_1 = 2(R + vt)/c$ in the phase of the above equation gives us

$$\phi_r - \phi_t = 2\pi \left( -f_c \left( \frac{2(R+vt)}{c} \right) + \frac{B}{2T} \left( \frac{2(R+vt)}{c} \right)^2 - \frac{B}{T} \left( \frac{2(R+vt)}{c} \right) t \right) \tag{1.15}$$

the second term in the equation has a $1/c^2$ dependency and can be neglected. Expanding the equation, we get

$$\phi_r - \phi_t = 2\pi \left( \frac{-2f_c R}{c} + \frac{2v f_c}{c} t + \frac{2BR}{Tc} t \right) \tag{1.16}$$

where $\frac{-2f_c R}{c}$ is the residual phase, $\frac{2BR}{Tc}$ is the beat frequency, $\frac{2v f_c}{c}$ is the Doppler frequency.

The additional processing to be done when converting a complex signal to real will be discussed in Chapter 2. The Anti-Aliasing Filter(AAF) will be removing the higher frequency components. We then convert our analog received signal to digital domain by using an Analog to Digital Converter(ADC). Since all simulations are done in MATLAB and considering the complexities that are involved while using ADC, the use of ADC is neglected for the system. We only consider a simple decimation filter which converts the received signal into samples of 40 MHz for processing the data.

Before doing an FFT to obtain range and doppler information, windowing is done over the fast time and sloe time samples to reduce the side lobes. This whole receiver chain and its respective blocks are shown in Fig 1.3
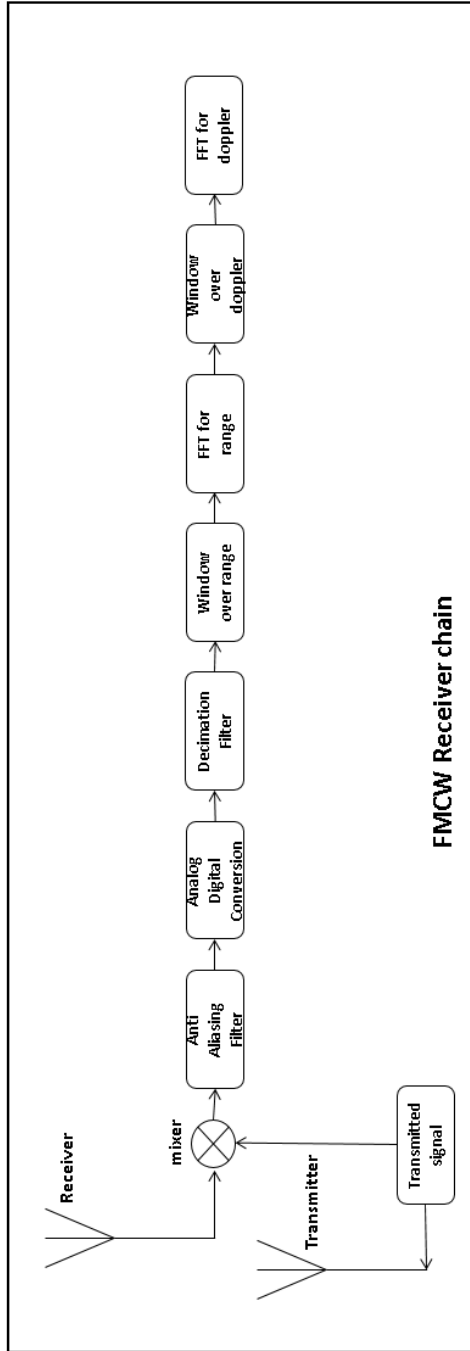
Figure 1.3: FMCW chain implemented

**1** 

## 1.7. PMCW SYSTEM INTRODUCTION

The Phase Modulated Continuous Wave(PMCW) radar works in principle different from the FMCW system. The typical equations for PMCW waveforms given in [6] are revisited here. In PMCW system, a modulated signal is divided into M bits, each having a duration of $t_b$ such that the total transmission time $T_P$ is given as

$$T_P = M t_b,  \tag{1.17}$$

with the condition that

$$u(t) = \sum_{m=1}^{M} \text{Rect}\left(\frac{t - (m-1)T_b}{T_b} exp(j\phi_m)\right),  \tag{1.18}$$

where $u$, is the m-th term of code and $\phi_m$ is the phase modulation(in radians) applied to the m-th term. A bi-phase code with phase states $\{0°, 180°\}$ yielding a code sequence consisting of elements $\{-1, 1\}$ is applied for this case.

The bi-phase MPS (Minimum Peak Side-lobes) codes, which include the Barker codes, achieve the lowest peak side to lobe ratio for a given sequence length. However, in many radar applications an optimum code is not absolutely required given that a "good" code with relatively low side lobe levels is available. Bi-phase maximum length sequences are used in radar applications as they provide predictable peak to side lobe ratios that approach 20log10(1/M) [7].

Since, we are concerned about interference in FMCW system due to PMCW system, we consider a simpler PMCW transmission system using Maximum Length(ML) sequence and try to understand the effects. The generation of the ML sequence is given as follows,

$$a_i = u_i a_{i-1} \oplus \text{u}_2 a_{i-2} \oplus ..... \oplus \text{u}_m a_{i-m}; \quad i = 1,..,2^{(m-1)}  \tag{1.19}$$

where $\oplus$ is modulo 2 addition. For our case, an initial ML sequence with a shift register of length 10 and with polynomials [10, 9, 8, 7, 5, 4] and [10, 9, 7, 5, 4, 2] are generated as these polynomials are predicted to have lower side-lobes than compared to the other polynomials. Generation of this sequence is as shown in Fig 1.4
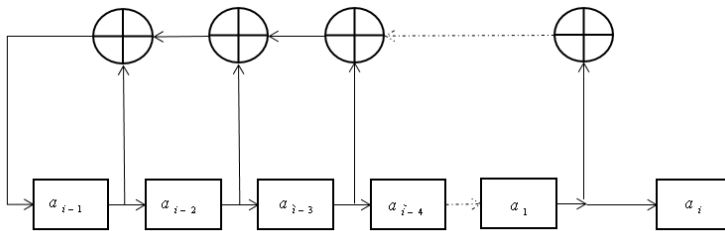


Figure 1.4: Generation of ML sequence

where $a_{i-1}, a_{i-2}, ..., a_1$ are the shift registers.

This generated sequence is multiplied with the carrier frequency to get the transmitted PMCW waveform

$$s_p(t) = \exp\left(2\pi f_p t\right) u(t), \tag{1.20}$$

where $s_p(t)$ is the transmitted PMCW signal, $f_p$ is the center frequency of the transmitted signal.

## 1.8. SUMMARY

In this chapter, We have described the fundamentals of Radars, along with uses of radars in automotive radar industry. Two important modulation schemes namely FMCW and PMCW for radars are described and also receiver chain for FMCW radar was described briefly. Since we are just going to use PMCW as an interferer in our thesis, we describe the basic transmission mechanism involved for PMCW system. With these descriptions, we instigate the interference problem in automotive radar. We subsequently describe our approach in solving this problem.

Most of the frequency domain descriptions in this thesis use a Short Time Fourier Transform (STFT) and spectrogram for better understanding of the relationship between frequency and time, it is to be understood when ever we talk about frequency and time dependency in the figures of transmitted and interference waveforms, it is a spectrogram that we are calculating. The analysis of spectrogram and STFT is described in detail in [8].

# 2

# STATE OF THE ART

In this chapter we look at the existing techniques to detect, identify and mitigate interference. The major step in mitigating interference is to first detect and identify the type of interference present. There are different counter measures proposed to overcome interference. A detailed study of existing detection, identification and mitigation techniques is presented in [9]. Most of the current detection and mitigation techniques detect the in-band interference energy. The disadvantages by doing this is that the interference can only be detected if the interference power levels are higher than the desired signal power. On the other hand, if the interference power is less than the multiple reflected signals there would be no point in trying to understand the impact of interference, this is why the interference power is considered to be similar or larger than the desired signal power.

The interference detection [10–13] and mitigation techniques that are currently present can be classified as pre-processing and post processing techniques. While pre-processing techniques in general would mitigate the interference in time domain of received signal before any processing is done to the received signal. The post-processing techniques rely on measuring the power spectral density(PSD) of target and interfering signals.

## 2.1. DETECTION AND IDENTIFICATION TECHNIQUES

In this section we discuss some of the detection and identification techniques, where they will be useful along with their advantages and disadvantages. As mentioned earlier, the mitigation techniques can be classified as pre-processing or post-processing techniques.

Techniques that deal with checking the sub-bands of the received digitized intermediate frequency(IF) are given in [10]. This type of detection techniques for interference can be placed just after digitization of the received signal. Interference can be mitigated after detection by any preferable mitigation techniques as described in later sections.

The detection techniques described in [10] try to detect the interference by comparing the instantaneous received power values with IF signal. The received signal strength

indicator (RSSI) values are calculated for the digitized IF signal and compared in the interference monitoring block. Four interference thresholds are specified after the interference monitoring component detects the power levels, these RSSI values for interference are quantized as E1, E2 and E3 levels, There are four possible interference detection

| RSSI | Impact |
|------|--------|
| <E1 | No interference |
| E1-E2 | Moderate interference,slight radar degradation |
| E2-E3 | High interference,medium radar degradation |
| >E3 | Severe Interference,no radar operation possible |

Table 2.1: Checking the values of RSSI as given in [10]

techniques described in this [10]. They can either be used independently or can be used in parallel for better detection of interference. These techniques are given as shown in the following figures
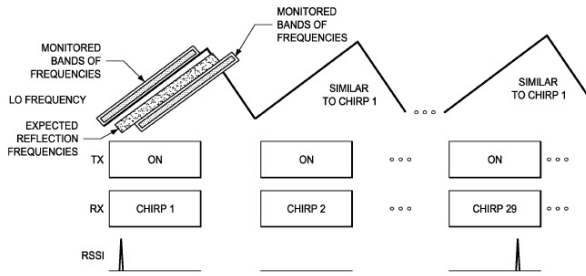


Figure 2.1: First method to detect interference as proposed by [10]

The first method to detect the interference as given in [10] is shown in Fig 2.1 , the first chirp in the sequence of the chirps to be sent is used to observe the interference signals. In that particular ramp the interference power level is measured, if there is interference in monitored bands of the frequencies the required mitigation technique is applied.
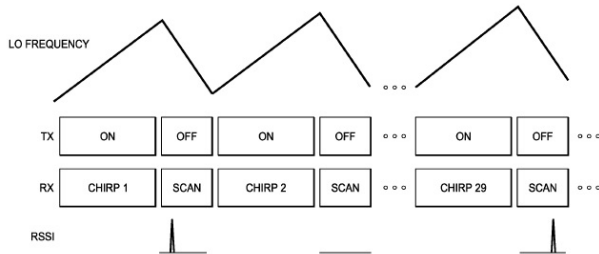


Figure 2.2: Second method to detect interference as proposed by [10]

In the second method, ramp down time is used to detect the interference. At this point transmitter is off but the receiver scans for the presence of any interference. This technique can also be used in parallel to the technique proposed in Fig 2.1 for better performance.
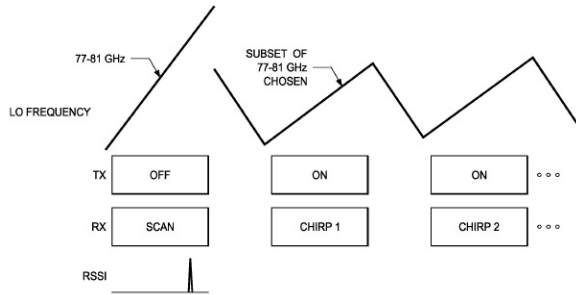


Figure 2.3: Third method to detect interference as proposed by [10]

In the third method, it is proposed that the first chirp of the transmitted ramp sequence will scan the whole of the available bandwidth for interference when the transmitter is turned off. The interference free sub-bands of frequencies will be detected from the first scan. The subsequent frame of chirps are then transmitted in the interference free sub-bands.
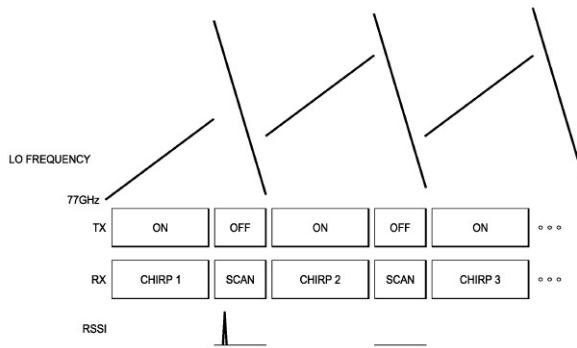


Figure 2.4: Fourth method to detect interference as proposed by [10]

The Fourth method proposed in [10] is more of a continuous scanning and detecting of interference. In the down ramp time, the received signal is scanned for interference in multiple sub-bands.

As these techniques consists of continuous scanning mechanism, it is required to put a lot of computational efforts other than the resources for object detection. Another disadvantage of these scanning methods is that we do not necessarily analyze the given interference signal. We would know the interference power but it is not necessary that the position of the interference can be detected in these techniques.

The next detection technique under study is [12], which does a frequency analysis over the beat signal. The FMCW radar device will calculate the value related to a sum of intensities of the frequency components, if this value is larger than a specified threshold, the FMCW radar device determines that it is an interfering signal from a nearby radar device. If the received multi-path signals have higher power than the interference signal, the device will consider them to be interference and might give a false alarm. It is also true that not many objects will have components in multi-path which has higher power than interfering signal itself, but if the transmit power of the interferer is very low, it is quite possible that the system will give a missed detection of interference as well.

In [14], the interference detection is done from comparing the beat signal obtained from the received spectrum. In this method, the extremal points within a period of the beat signal is measured.
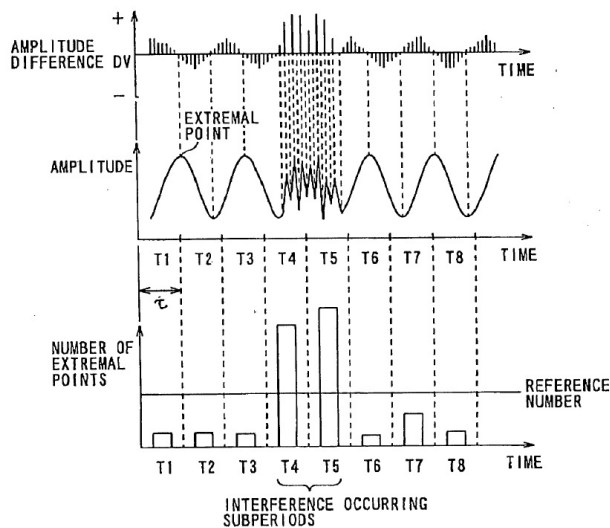


Figure 2.5: method to detect interference as proposed by [14]

In general if there is no interference, there would be only two extremal points in a single period. But when there is an interference, there would be more than two extremal points as shown in Fig 2.5. We can observe that the maximal points in the beat signal is constant and less than the reference number (above which an interference is detected) when there is no interference. But when there is an interference, the beat signal has a very high distortion and the number of extremal points in that sub-period go beyond the reference number.

There is an underlying assumption in this method that the interfering signals have harmonic components which are very different from the received radar. So the occurence of interference can be very well detected in this case without a lot of computational efforts. If the interfering signal is coherently added with the transmitted signal, this results in ghost targets or corruption of whole of the beat signal interval. (generally happens when both the radars operate with similar slope and are in the same frequency sub-band), the

detector will not consider this situation as an interference.

Another time domain interference detection technique is given in [13]. Even this interference detection is only for the interference signals which are relatively small compared to the received signal. A Constant False Alarm Rate (CFAR) is used over the time domain received signal to detect the presence of interference. Post detection of interference, the interference will be mitigated by using a band-stop filter. The performance of this technique is as shown in Fig 2.6
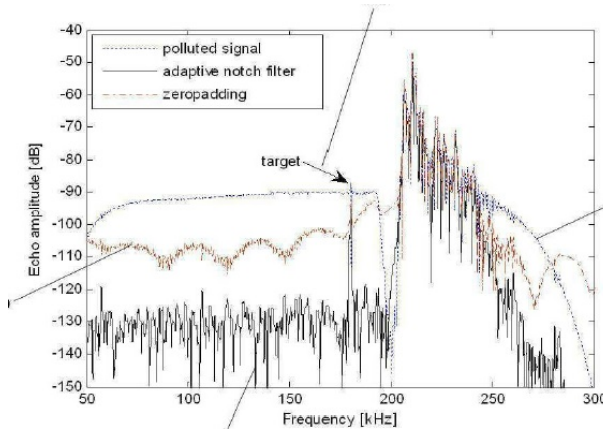


Figure 2.6: method to detect interference as proposed by [13]

Even in this technique, we observe that the interfering signal, which has a power level higher than the received signal will be perceived as a target rather than interference.

## 2.2. MITIGATION/AVOIDANCE TECHNIQUES

It is required to mitigate/avoid the interference, if the interfering signal is distorting the received signal. There are several domains in which mitigation/avoidance techniques can be applied on automotive radar [9]. Polarization domain in which the transmitter is designed to have a specific polarization from the other radar transmitters in linear, circular or cross polarization so that interference in one polarization can be avoided by another polarization, Time domain in which the duty cycle of the transmitted FMCW wave can be modified to avoid the interference or to use a random time modulation of the frequency(by pausing transmission), Frequency domain techniques suggests to randomly hop into the frequency sub-bands which are not affected by interference. Coding techniques which suggest using a device specific code to achieve orthogonality for each of the device. Also Spatial domain techniques which suggest beam forming to mitigate the interference can be used for mitigation . Strategic techniques which detect and repair or change frequency are also very prevalent in the current automotive radar scenario. Some of these described mitigation techniques are discussed in detail in the following section. We analyze their advantages, dis-advantages and their limitations.

### 2.2.1. TIME DOMAIN MITIGATION TECHNIQUES

A systematic view on the how the interference will occur and the methods to counter the interference effects is given in[15]. When the value of the peak is higher than the assigned CFAR threshold, the interference is detected. It is suggested that the interference can be mitigated by replacing the affected samples with null in time domain and try to regain the lost dynamic range in frequency domain.

A simple and basic mitigation is to null the interference affected samples [16], but this leads of widening of peaks in the spectrum. For better performance of this method, a windowing scheme can be applied, which will smoothen the edges reducing the widening of the peaks. It is also suggested that the use of notch filter and linear prediction of the samples given as

$$x(n+1) = \sum a(k).x(n-k+1)$$

where $x(n+1)$ is the predicted state of the sample, $a(k)$ is windowing coefficient applied and$x(n-k+1)$ is the previous state of the sample, will suppress the interferer. The actual beat signal is re-constructed over the part of interference affected samples by the linear prediction model. It was also suggested that interference detection can be done in time-frequency domain , by using the time-frequency Short Time Fourier Transform (STFT), the signal can be resolved in several frequency bands. In any of the bands, a long chirp can be treated as a localized(short) disturbance which can be detected. In general this time domain nulling would lead to a significant gain in Signal to Interference plus Noise Ratio(SINR), but this method would not be really useful when the interference is distributed along many samples. Also, due to this nulling, side-lobes will be very evident which are not so desirable. This problem of nulling side lobes is addressed in [17]. In the proposed method, interference is considered to have a higher amplitude than the signal itself. As a result the phase of the received signal would have a dominant interference component. The phase response of the received signal given as

$$\frac{d}{dt}s_{rx}(t) \approx -A_{int}\sin(\phi(t))\frac{d}{dt}\phi(t)$$

where $s_{rx}(t)$ is the received time domain signal, $\phi(t)$ is the phase shift of the interfering signal. It was suggested to mitigate the interference signal by subtracting the estimated interference component. Further details of this mitigation technique can be studied in [17]. The advantage of this technique is that no information of the actual received signal is lost and with the parameters estimated, the interference period can be calculated. But the achievable SINR gain is limited as perfect estimation of the interference is not possible and also even in this technique, interference signal is considered to have higher amplitude than the beat signal.

### 2.2.2. SPATIAL DOMAIN MITIGATION TECHNIQUES

The technique used in [18] is a digital beamforming in spatial domain. The best known application of Digital beamforming is to estimate the direction of arrival. In this method the interference is detected when the average energy considered in a time frame rises above a given threshold. When the interfering samples are detected, the interference covariance matrix $Q$ is determined from the identified interference sequence $y_i[k]$ and $S$

snapshots of the received signal.

$$\widehat{Q} = \frac{1}{S} \sum_{s=1}^{S} y_s y_s^* = \frac{1}{S} Y Y^*$$

A noise matrix is added to reduce the influence of the eigen value fluctuation

$$\widehat{Q} = \frac{1}{S} Y Y^* + \alpha I$$

where, $\alpha$ is a loading factor and $I$ is the identity matrix. This would also ensure that the estimated co-variance matrix is non-singular hence invertible. The interference is suggested to be suppressed by computing the angular spectrum $\hat{x}[k]$ as

$$\hat{x}[k] = A^* \widehat{Q}^{-1} x[k]$$

where $A$ is the transformation matrix. This is called Loaded Sample Matrix Inversion(LSMI). Another spatial domain mitigation technique is suggested in[19]. When I-Q mixer is not present, it is not enough to cancel the DOA of an interferer alone, a second DOA (which is the image of the actual DOA of interferer) must also be blinded. This technique uses simple beam forming to cancel both the DOA of the interferer. When no I-Q mixer is used, the base band signal is of the form

$$\cos(x) = \frac{1}{2}(e^{jx} + e^{-jx}).$$

This signal would produce two peaks in the frequency domain, so nulling in both directions is needed. Weights of the beam former are chosen such that the interfering signal is canceled in both directions.

$$w_1 S_{int1}(f) + w_2 S_{int2}(f) = 0$$

It was also proved that the second DOA is exactly that of an interferer but opposite in direction. It was claimed that, an interference induced of 15dB to be suppressed in from the spectrum and SNR improvement of 40dB is achievable. These algorithms would require going into the matrix sub-space domain of the signal, it would take up more resources in signal processor. Note that if the interference is too weak, the suppression would make no sense since the power is spread across the whole range profile and has little effect on reasonably strong targets.

### 2.2.3. CODING DOMAIN MITIGATION TECHNIQUES

In [20], a method to mitigate the FMCW interference in coding domain is given. A coded stepped -FMCW signal for automotive radar is proposed. The FMCW waveform consists of two slope pairs and can be divided into for segments in one cycle. Each segment is modulated with a PN-code to have a good anti-interference capability. Fig 2.7 describes the method proposed in[20].
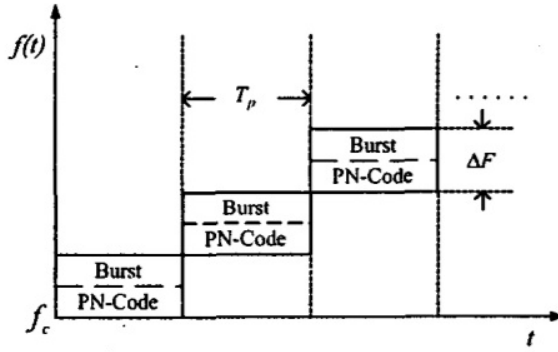
Figure 2.7: method to mitigate interference as proposed by [20]

In Fig 2.7, $T_p$ is the ramp up/down time, $\Delta F$ is the bandwidth of each of the segment, $f_c$ is the carrier frequency and $f(t)$ is the instantaneous frequency.

It is assumed that each vehicle is equipped with a different PN (Pseudo Noise)-code modulated approach so that each vehicle has a unique PN code for transmission. When a car which is equipped with another PN-code interferes with the victim, the resultant phase of the base-band pulse is random. So this out of phase interference can be easily removed while processing. This is in-fact an interesting technique considering the advantages in mitigating interference, but in existing automotive radar scenario, having a distinct transmit code for each vehicle might not be a feasible solution.

### 2.2.4. STRATEGIC MITIGATION TECHNIQUES

These techniques mitigate the interference signal, after processing the received data. The detection or identification of the interference can be done in pre-processing or post-processing stage. These are the most prevalent and expansive techniques under study. Most of the discussed mitigation techniques until now can be used strategically in tandem for better performance. Some of the mitigation techniques post detection in this domain are given as follows.

In[21] a method for mitigating the interference post-processing using a maximally stable extremal regions(MSER) [22] is proposed. The regions found by the MSER algorithm are stored as a binary pattern image $P \in (0,1)^{M.N}$. It will be stored as 1 for a disturbed sample and 0 for undisturbed sample. If a specified number of samples are corrupted then the whole measurement is to be considered as corrupted. After the detection of interference, the post-processing mitigation techniques can remove the interference. It was suggested to apply an inverse raised cosine window at locations of the disturbed signals to avoid ringing artifacts when computing the DFT afterwards. This technique uses image processing techniques over the time-frequency domain. However, the computational complexity and additional hardware required for this system is not completely described for this method.

### 2.2.5. Avoidance using frequency hopping

In [23], a frequency hopping mechanism inspired by bats is studied. Interference detection is performed over the baseband signal of each ramp with a power detector. A decision is made by knowing if the interfered frequencies are detected above or below the center frequency. The center of interference is calculated similarly to the center of mass of a homogeneous object as

$$\hat{r} = \frac{1}{N_{int}} \sum_{i=1}^{N_{int}} \frac{s_i}{N}$$

where, $\hat{r}$ is the estimated center of interference , $N$ is the total number of samples in a frequency ramp, $s_i$ is the numbers of the interfered samples in a single beat signal and $N_{int}$ is the number of affected ramps. For example, if the interference center is at 256th sample over 5 ramps which has 1024 samples each then

$$\hat{r} = \frac{1}{5} \sum_{i=1}^{5} \frac{256}{1024}$$

giving $\hat{r} = 0.25$, which would imply that the shift has to be upwards.
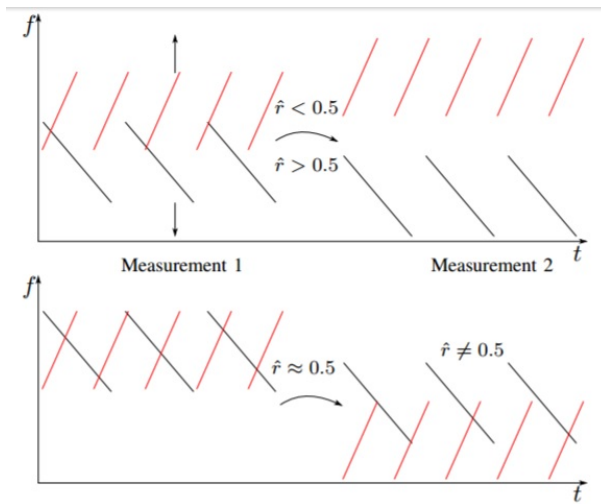


Figure 2.8: method to mitigate interference as proposed by [23]

As shown in the Fig2.8 a decision is made to hop to higher frequencies if $\hat{r} > 0.5$ or a decision is made to hop to lower frequencies if $\hat{r} < 0.5$. There is an obvious problem when $\hat{r} = 0.5$, a clear decision can not be made. Also, if the bandwidth of the interference is higher than the transmitted signal, hopping to a frequency band above or below the current frequency band might not avoid the interference. In this case a single jump might not be sufficient as the interference might affect the transmitted ramp again.

## **2.3.** SUMMARY

In this chapter, we have discussed about the existing detection, identification, mitigation and avoidance techniques. We have detailed the procedure that these techniques follow and discussed about the advantages and dis-advantages of these methods. We have distinguished these techniques as pre-processing and post-processing techniques. We choose to further investigate on strategic mitigation techniques such as detect and avoid/mitigate as they have the best suppression of interference. In the forthcoming chapters we develop our detect/identify and mitigate technique and evaluate its performance.

# 3

# INTERFERENCE

## 3.1. INTERFERENCE IN AUTOMOTIVE RADAR

Interference occurs when two waves are propagating simultaneously in the same media. These waves can add up either constructively or destructively in this medium. Interference might attenuate the performance of any wireless system including automotive radar. In an automotive radar, a significant deterioration in performance is due to the mutual interference between the automotive radars when they are in close proximity. This mutual interference has to be mitigated to for the better performance of automotive radars. Two types of phenomena occurs in the presence of mutual interference namely, appearance of ghost targets if there is a presence of a correlated interference and reduced sensitivity in the presence of uncorrelated interference (which increases noise floor) [2],[3] gives more insight into these phenomena.

### 3.1.1. WHAT IS THE PROBLEM?

There are going to be about 6-8 radars on a car for making it safer for the passengers. As the number of radars that are equipped in a car keeps increasing, it is likely that there exist mutual interference among radars equipped on the same car and also between radars of different cars. The scenario of this thesis is more inclined towards observing the effects of mutual interference between radars when a single radar is placed on all the vehicles. This study is confined to the simulation of three basic mutual interference scenarios for radars present in the real world.

First case is a FMCW system that is acting as an interferer. Phase Modulated Continuous Wave radar has been accruing some interest in research lately. It is also a concern in the industry if there is any interference from PMCW to an FMCW system. The second scenario deals with the presence of PMCW interferer. Third scenario, is a simple continuous wave interferer.

The three interference scenarios, which we will be looking into in this thesis, will be discussed in the following sections.
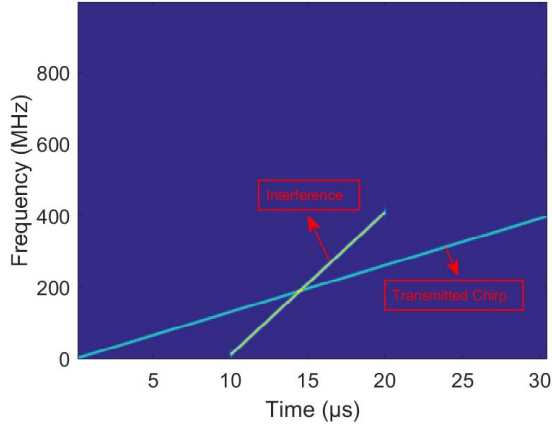
Figure 3.1: FMCW against FMCW interference

## FMCW AGAINST ANOTHER FMCW SYSTEM

The first case of interference under study is where two FMCW systems interfere with each other. For this case, we have considered a transmitted chirp of 400 MHz Bandwidth and a transmit time of $30.6\mu s$. Interfering signal is considered from another FMCW system with a bandwidth of 400MHz and a transmit time of $10\mu s$. We can clearly see that the instantaneous frequencies of these two chirps in this case overlap each other at about $15\mu s$. The prediction on how noise floor will be increased will be studied later in this chapter. If the slopes of these transmit and FMCW system are same and if the interfering signal is in the range of anti-aliasing filter's cut off frequency, we would observe a ghost target because interfering chirp would be processed as the received reflected signal, giving an object that is non-existent. This would lead to an obvious problem since the objects which are not present in reality will be detected.

## FMCW AGAINST PMCW SYSTEM

Phase Modulated Continuous Wave (PMCW) radar is under extensive research in the automotive radar domain. It is claimed to be inherently robust against interference because of its cross correlation properties. For our case, PMCW radar is essentially a coded radar operating at the same center frequency as that of the FMCW radar. So this might lead to interference which is to be investigated and if it has a potential to reduce the efficiency of FMCW system. This PMCW interference affects mostly when spectral peak of transmitted signal of the PMCW signal is in band to the FMCW system. Considering a narrow band PMCW system, the spectrum of PMCW signal generated is shown in Fig 3.2. The impact of PMCW signal interfering with the FMCW system with a bandwidth 400 $MHz$ and transmit time of $30.6\mu s$ having the same center frequency is shown in Fig 3.3. It is evident from Fig 3.2 that if the main lobe of the PMCW interferer is in band with the transmitted FMCW chirp, the interference level should be atleast 13 dB higher than the case when it is not. So as a worst case scenario, we consider the main lobe to be in band for the transmitted FMCW chirp.
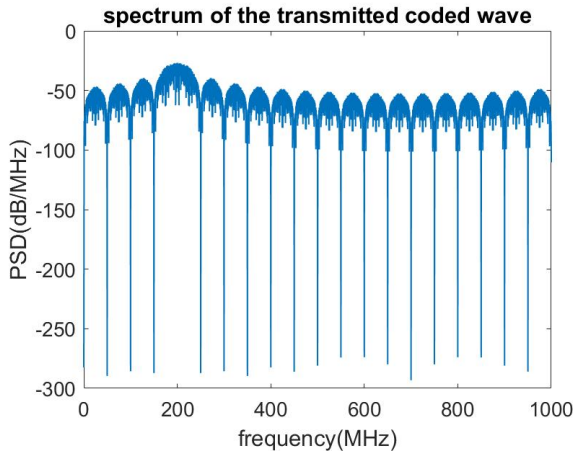
Figure 3.2: PMCW waveform
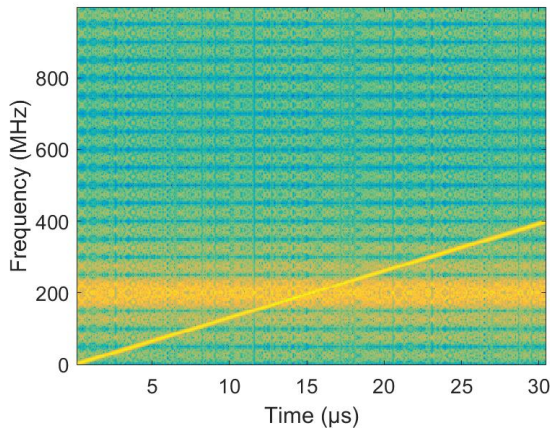


Figure 3.3: PMCW against FMCW interference

### FMCW AGAINST CONTINUOUS WAVE(CW) SYSTEM

In the presence of a Continuous Wave interferer, the spectrum of a CW would be con-
centrated over a single frequency. So the CW interferer would effect the maximum when
the frequency of the CW is equal to the FMCW wave interferer. This type of interferer
shapes like a spike in time domain. The Spectrogram which depicts the CW interferer
with a center frequency of 200 $MHz$ interferer against an FMCW system of bandwidth
400 $MHz$ and transmit time of 30.6$\mu s$ is shown in Fig 3.4.
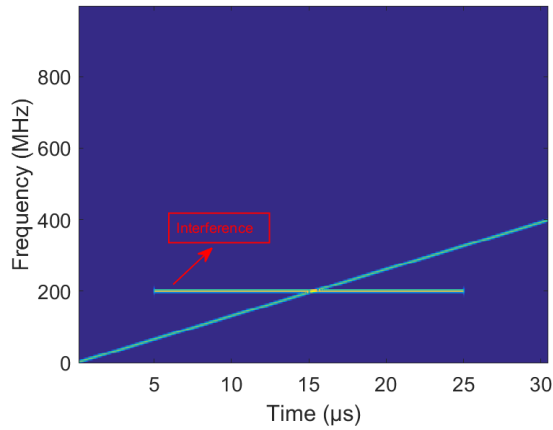
Figure 3.4: CW against FMCW interference

### 3.1.2. ASSUMPTIONS AND LIMITATIONS

It is assumed that FMCW ramp is completely linear. Also receiver is assumed to be working in linear mode, i.e the receiver power from interference will not saturate the receiver. For better understanding of the problem, we consider ideal low pass and high pass filters. Most of the equations that will be derived in the thesis will be by taking FMCW and CW cases only, these equations could be extended for a PMCW case when the PMCW interferer is in band to the FMCW transmit chirp. But the detailed study on PMCW and its effect on FMCW is suggested for further research. Most of our analysis consists of a single interferer cases, mitigation in presence of multiple interferer is open for future work.

### 3.1.3. SIMULATION PARAMETERS

A calculation of the signal propagation in the presence of a single interferer and parameters selected are as shown in the Table 3.1. The calculations for desired (D) to undesired signal(U) are summarized from, [24].

| Parameters | Values |
|:---:|:---:|
| center frequency ($f_c$) | 79 GHz |
| distance(d) | 50 m |
| transmit power($P_t$) | 10dBm |
| Noise Figure($NF$) | 15dB |
| Transmit Gain ($G_t$) | 12dB |
| Receive Gain ($G_r$) | 12dB |
| Number of samples per ramp(N) | 1024 |
| Radar Cross Section(RCS) | 10 dBsm |
| ADC sampling frequency($f_{samp}$) | 40 MHz |

Table 3.1: Parameters chosen for calculation of the SNR in the presence of a single interferer

## 3.2. PATH LOSS MODEL

For our case, a desired signal(D) is reflected from the target and an undesired signal (U) is the one that has a direct path from the interferer as shown in Fig 3.6. Noise Figure ($NF$) for our system is assumed to be 15 dB and further noise calculations are given as follows Noise power is calculated from formula

$$\eta = KT_0B, \tag{3.1}$$

where, $K$ is Boltzmann constant, $T_0$ is temperature and $B$ is the effective Bandwidth in which noise is present. Since $K$ is a constant and considering room temperature 300 $K$, the noise Power Spectral density can be calculated just by taking $\eta_{PSD} = KT_0$ this gives a value of $-174$ *dBm/Hz*. Operational bandwidth of noise is to be multiplied with noise PSD to give actual noise power that is present in the system. This can be written in *dBm* as,

$$\eta = -174 + NF + 10\log(f_{samp}) \tag{3.2}$$

depending on the selected $f_{samp}$, we will have the integrated noise power entering our system equivalent to this value. For our case with the parameters in Table 1, we get

$$\eta = -88dBm = -118dB$$
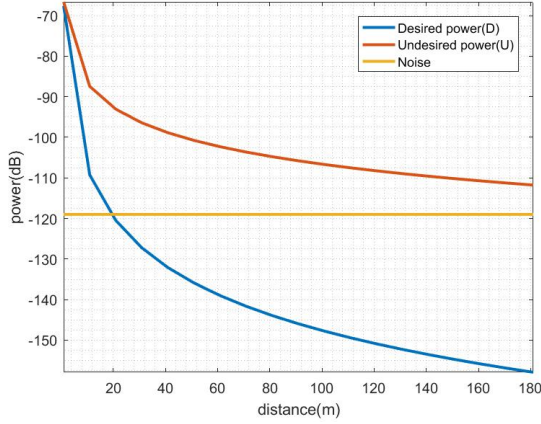
Figure 3.5: Path loss model for calculating desired and undesired signal power

For a test case of the object and interferer at 10 m, the calculations for the desired and undesired signal are given as follows.

The received power for the undesired signal from the path loss model is given as

$$P_U = P_t G_t G_r \left( \frac{\lambda}{4\pi d} \right)^2 \tag{3.3}$$

in log scale , the signal to noise ratio(SNR) for the undesired signal ($U_{SNR}$) is given as

$$U_{SNR} = P_t + G_t + G_r + P_L - \eta \tag{3.4}$$

Where, $P_L = 20log(\frac{\lambda}{4\pi d})$ with the parameters given in Table 3.1 , we get the following values

$$U_{SNR} = -10 + 12 + 12 + 20log\left( \frac{\lambda}{4\pi d} \right) - (-118)$$

$$U_{SNR} = 41.3 dB$$
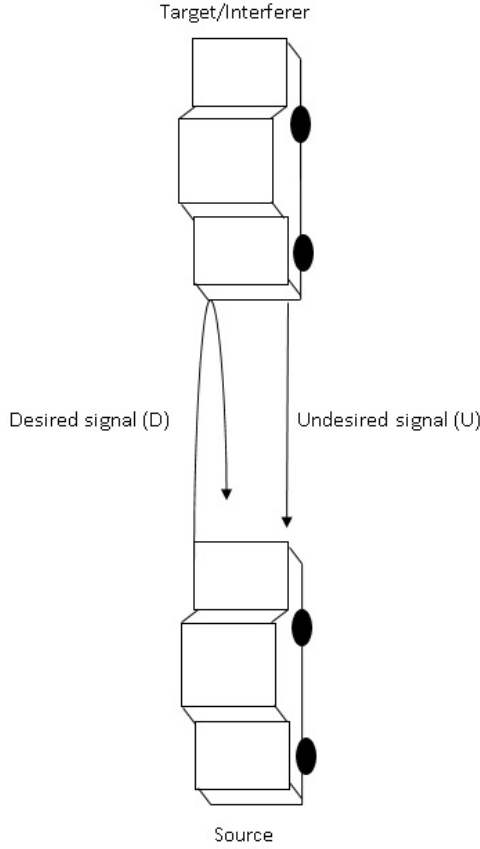
Figure 3.6: Simple propagation model for link budget calculations

The desired signal is the one that is reflected from the other object, this will give an additional RCS dependent term.
The signal power for the desired signal ($P_D$) is given as

$$P_D = \frac{P_t G_t G_r \lambda^2 \sigma}{(4\pi)^3 d^4} \tag{3.5}$$

in log scale , the SNR for the desired signal ($D_{SNR}$) is given as

$$D_{SNR} = P_t + G_t + G_r + 10 log\left(\frac{\sigma}{4\pi d^2}\right) + P_L - \eta \tag{3.6}$$

The desired signal SNR is then found out to be

$$D_{SNR} = 20.3\text{dB}$$

So the desired to undesired signal power ratio from the parameters in Table 1 is given as

$$DUR(\text{dB}) = D_{SNR} - U_{SNR} = 10 log\left(\frac{\sigma}{4\pi d^2}\right) = -21\text{dB}. \tag{3.7}$$

where, $\sigma$ is the radar cross section(RCS) and $d$ is the distance of the target/interferer from the source.In general , the $DUR$ is expected to be positive to detect a target. But, we can clearly see that the Undesired signal power is much higher than that of the desired signal power which masks out the target itself. Fig 3.5 shows desired (D) and undesired signal (U) powers. Since undesired signal has a inverse relationship with $d^2$ where as desired signal has an inverse relationship with $d^4$. Hence the Desired Signal power falls off faster than the Undesired Signal power. We can also observe from 3.5 that interference power exceeds the noise power which might degrade the sensitivity of our system. In the receiver chain, this difference in power for desired to undesired signal power might mask out the desired signal itself. That is why there is a need to mitigate this undesired (interference) signal so that desired signal is not masked.

## 3.3. INTERFERENCE IN TIME DOMAIN

The equations for transmission and reception of the FMCW radar are given in the previous chapters, over here we revisit them to further describe our approach in detection, identification and signal separation for mitigation. The transmitted signal is given as

$$s_t = \text{Rect}\left(\frac{t - T/2}{T}\right) \exp\left(2\pi j(f_c t + \frac{S_1 t^2}{2})\right) \tag{3.8}$$

where $S_1$ is slope of transmitted signal given as $S_1 = \frac{B}{T}$ and $f_c$ is the center frequency. The received signal will have two signals components from the reflection of object and the interference.

$$s = s_r + s_i, \tag{3.9}$$

where $s_r$ is the received reflected signal component and $s_i$ is the interference component and $s$ is the total received component.

$$s_r = A_r \text{Rect}\left(\frac{t - T/2 - \tau_1}{T}\right) \exp\left(2\pi j(f_c(t - \tau_1) + \frac{S_1}{2}(t - \tau_1)^2)\right) \tag{3.10}$$

where $A_r = \sqrt{P_r}$ is the amplitude, $P_r$ is the power of the received reflected signal component and $\tau_1$ is the round trip delay. Interferer on the other hand is assumed to have a different slope($S_2$) than that of a transmitted signal

$$s_i = A_i \text{Rect}\left(\frac{t - T_i/2 - \tau_2}{T_i}\right) \exp\left(2\pi j(f_i(t - \tau_2) + \frac{S_2}{2}(t - \tau_2)^2)\right) \tag{3.11}$$

where $S_2$ is the slope of the interferer, $f_i$ is the center frequency of the interferer and $\tau_2$ is the time delay for the interferer with respect to transmitted chirp, $A_i = \sqrt{P_i}$ is the amplitude $P_i$ is power of interferer. The received signal is down converted at the mixer with conjugate of transmitted signal, mixer equation is given as

$$s_m = s s_t^* \tag{3.12}$$

The down converted signal is given as

$$s_m = \text{Rect}\left(\frac{t - T/2 - \tau_1}{T - \tau_1}\right)\left(A_r \exp(\pi j(S_1\tau_1^2 - 2S_1 t\tau_1 - 2f_c\tau_1)))\right)$$
$$+ \text{Rect}\left(\frac{t - T_i/2 - \tau_2}{T_i}\right)\left(A_i \exp(\pi j((S_2 - S_1)t^2 + S_2\tau_2^2 - 2S_2 t\tau_2 - 2f_i\tau_2 - 2(f_i - f_c)t)\right)$$
$$(3.13)$$

this can be simplified into

$$s_m = s_{mr} + s_{mi} \tag{3.14}$$

where $s_{mr}$ is the received reflected signal component and $s_{mi}$ is the received interference signal component.

An analog low pass filter is used to remove the images obtained from the mixing process and acts as an anti-aliasing filter(AAF) for subsequent analog to digital conversion. We have considered a wide band interference post down conversion in intermediate frequency (IF),so we need to optimize the design of LPF so that the impulse response and group delay of the filter does not introduce any additional artifacts that affect the performance of detection and identification in our algorithms.

We initially consider a perfect Brick wall filter as the LPF whose transfer function $H(f)$ is given as follows.

$$H(f) = \text{Rect}\left(\frac{f}{2f_{LPF}}\right) \tag{3.15}$$

where $f_{LPF}$ is cut off of the LPF and $f$ is the instantaneous frequency of the input signal Looking at this instantaneous frequency which is obtained by differentiating the phase of the received interference signal,

$$\frac{1}{2\pi}\frac{d\phi_i}{dt} = \left((S_2 - S_1)t - S_2\tau_2 - (f_i - f_c)\right) \tag{3.16}$$

where, $\phi_i$ is the phase of the interference signal post down conversion. This instantaneous frequency is linearly dependent in time, when we apply a LPF onto the received signal, the higher frequency terms will be cut off implying that the interference is actually band limited by the LPF. The limits are given as follows

$$-f_{LPF} \leq \left((S_2 - S_1)t - S_2\tau_2 - (f_i - f_c)\right) \leq f_{LPF} \tag{3.17}$$

the total time for interference is the time interval in which the instantaneous frequency of down converted interference goes from $-f_{LPF}$ to $f_{LPF}$ as given in [4].

$$T_i = \frac{2f_{LPF}}{S_2 - S_1} \tag{3.18}$$

where $T_i$ is the total time for which interference is present. So the received interference signal post LPF is given as

$$s_{ml} = \begin{cases} s_{mi} & \frac{-f_{LPF} + 2S_2\tau_2 + (f_i - f_c)}{(S_2 - S_1)} \leq t \leq \frac{f_{LPF} + 2S_2\tau_2 + (f_i - f_c)}{(S_2 - S_1)} \\ 0 & otherwise \end{cases} \tag{3.19}$$

where $s_{ml}$ is the interference limited by the LPF and

$$s_{mi} = \text{Rect}\left(\frac{t - T_i/2 - \tau_2}{T_i}\right)\left(A_i\exp(\pi j((S_2 - S_1)t^2 + S_2\tau_2^2 - 2S_2 t\tau_2 - 2f_i\tau_2 - 2(f_i - f_c)t))\right)$$
(3.20)

For better understanding of how this interference is localized due to the LPF, a rectangular function is used

$$s_{ml} = s_{mi}\text{Rect}\left(\frac{t - t_{center}}{\frac{2f_{LPF}}{S_2 - S_1}}\right)$$
(3.21)

where $t_{center} = \frac{2S_2\tau_2 + (f_i - f_c)}{(S_2 - S_1)}$ is time instant where instantaneous frequency of interferer is equal to the instantaneous frequency of transmitted signal. The use of this time instant and way to estimate this is shown in Chapter 5. Also the argument of exponential of (3.20) is in the form of $y = ax^2 + bx + c$ which is nothing but a generic equation of a parabola more detailed study on how this equation unfolds the information related to the interferer is given in [17].

Fig 3.7 gives a depiction of the noise power spectral density post mixing (3.20) and post LPF (3.19). We can see that the integrated noise power is reduced by using LPF and also observe the magnitude response of our LPF. We have considered a Bandwidth of 400 Mhz for interferer and a LPF of 10 MHz cut off.
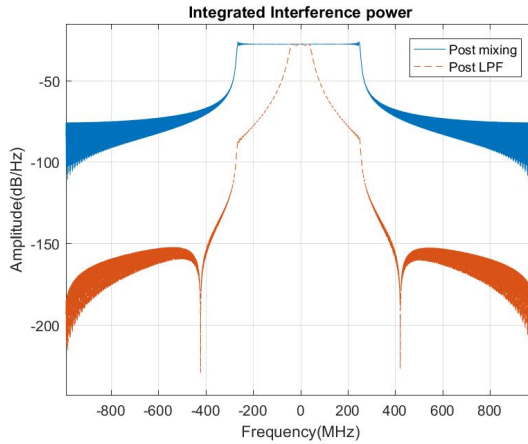


Figure 3.7: Integrated Noise power

In Fig 3.8, we can see that the AAF has localized our interferer to a window ranging from $12\mu s$ to $18\mu s$. With this information , we try to localize interference using a rectangular window as described in (3.21).
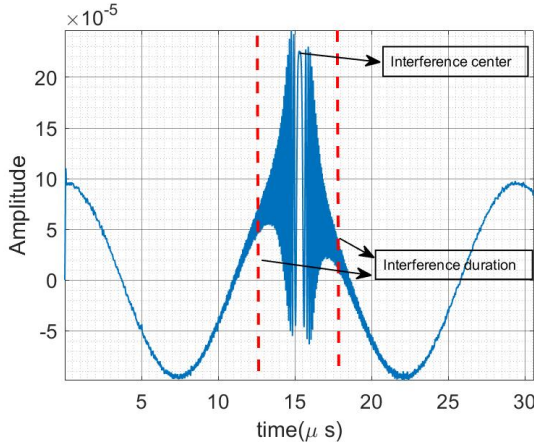
Figure 3.8: Interference is shown to be localized in $12\mu s$ to $18\mu s$ and has a center at $15\mu s$ because of the LPF from (3.21)

## 3.4. ANALYSIS OF RECTANGULAR FUNCTION

In, this section we analyze the properties of rectangular function specific for our case. Interference over the received reflected signal in Fig 3.8 can be localized using rectangular functions as follows.
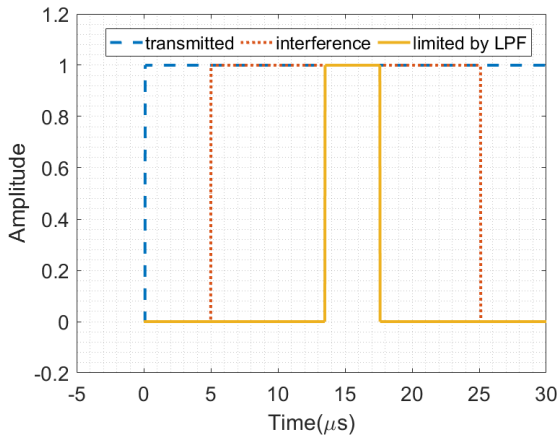


Figure 3.9: Rectangular function analysis

In Fig 3.9, we look into the rectangular functions that we have used in understanding the localization of interference. The transmitted chirp will be a combination of rectangular function $\text{Rect}\left(\frac{t-T/2}{T}\right)$ in the range $(0, T)$. The interference is given as $\text{Rect}\left(\frac{t-T_i/2-\tau_2}{T_i}\right)$ in the range $(0, T_i)$. Post LPF, interference is time limited by the cut off frequency of the LPF. So, a new rectangular function which corresponds to the range $-\left(\left(\frac{f_{LPF}}{S_2-S_1}\right),\left(\frac{f_{LPF}}{S_2-S_1}\right)\right)$

is given as $\text{Rect}\left(\dfrac{t-t_{center}}{\frac{2f_{LPF}}{S_2-S_1}}\right)$. If we multiply the rectangular function limited by LPF with the rectangular function of interference then the resultant will be the rectangular function limited by LPF itself. Hence, the interference can be localized by the use of rectangular function.

## 3.5. INTERFERENCE IN FREQUENCY DOMAIN

Interestingly, this equation of parabola (3.20) can be translated to another equation of chirp by simply taking $\tau_2 = 0$ and considering center frequencies $f_c = f_i$ implying that transmitted and interfering signal have a same start time and center frequencies. This equation for chirp has been solved in [25]. For our case we solve it without any prior assumptions to understand the interference behavior in frequency domain. By doing this, the received chirp is just shifted up or down in frequency. Now when we do the FFT to obtain the range information. The down converted interference post in Frequency domain will be spread over the whole of frequency band as shown in this section. We take the simple analog signal (3.20) and perform a Fourier transform to understand how the interferer would look like in frequency domain.

$$S_i(F) = \int\limits_{-T_i}^{T_i} \exp^{\left(\pi j((S_2-S_1)t^2+S_2\tau_2^2-2S_2t\tau_2-2f_i\tau_2-2(f_i-f_c)t)\right)}\exp^{(-2j\pi f t)}dt \tag{3.22}$$

where $S_i(F)$ is the frequency spectrum of down converted interference, $T_i$ is the time for which interference is present

$$S_i(F) = \exp^{\pi j\left(S_2\tau_2^2-2f_i\tau_2\right)}\int\limits_{-T_i}^{T_i} \exp^{\pi j\left((S_2-S_1)t^2-2(S_2\tau_2+(f_i-f_c))t\right)}\exp^{(-2j\pi f t)}dt \tag{3.23}$$

Considering $\Delta S$ to be difference in slopes $\Delta S = S_2 - S_1$

$$S_i(F) = \exp^{\pi j\left(S_2\tau_2^2-2f_i\tau_2\right)}\int\limits_{-T_i}^{T_i} \exp^{\pi j\left(\Delta St^2-2(S_2\tau_2+(f_i-f_c))t\right)}\exp^{(-2j\pi f t)}dt \tag{3.24}$$

$$S_i(F) = \exp^{\pi j\left(S_2\tau_2^2-2f_i\tau_2\right)}\int\limits_{-T_i}^{T_i} \exp^{\pi j\Delta S\left(t^2-2\frac{(S_2\tau_2+(f_i-fc)-f)}{\Delta S}t\right)}dt \tag{3.25}$$

$$S_i(F) = \exp^{\pi j\left((S_2\tau_2^2-2f_i\tau_2)-\frac{((S_2\tau_2+(f_i-fc)-f)^2}{\Delta S}\right)}\int\limits_{-T_i}^{T_i} \exp^{\pi j\Delta S\left(t-\frac{(S_2\tau_2+(f_i-fc)-f)}{\Delta S}\right)^2}dt \tag{3.26}$$

Solving the integral term only,

$$\int\limits_{-T_i}^{T_i} \exp^{\pi j\left(\sqrt{\Delta S}\left(t-\frac{(S_2\tau_2+(f_i-fc)-f)}{\Delta S}\right)\right)^2}dt \tag{3.27}$$

Let

$$\sqrt{\Delta S}(t - \frac{(S_2\tau_2 + (f_i - f_c) - f)}{\Delta S}) = x; dt = \frac{dx}{\sqrt{\Delta S}}$$

so the integral can be written in terms of x as

$$\int_{-X_1}^{X_2} \exp^{\pi j x^2} \frac{dx}{\sqrt{\Delta S}} \tag{3.28}$$

the above equation is a fresnel integral equation where $X_1$ and $X_2$ are given as

$$X_1 = \frac{\Delta S T_i + (S_2\tau_2 + (f_i - f_c) - f)}{\sqrt{\Delta S}}$$

$$X_2 = \frac{\Delta S T_i - (S_2\tau_2 + (f_i - f_c) - f)}{\sqrt{\Delta S}}$$

so the integral can be written in the form of fresnel coefficients as

$$\frac{[C(X_1) + jS(X_1) + C(X_2) + jS(X_2)]}{\sqrt{\Delta S}} \tag{3.29}$$

Let us consider the case of CW interference so that $S_2 = 0$ and $\Delta S = -S_1$ so that the limits of integral $X_1$ and $X_2$ are given as

$$X_1 = \frac{-S_1 T_i + ((f_i - f_c) - f)}{\sqrt{S_1}} \tag{3.30}$$

$$X_2 = \frac{-S_1 T_i - ((f_i - f_c) - f)}{\sqrt{S_1}} \tag{3.31}$$

substituting $S_1 = \frac{B}{T}$ and considering

$$X_1 = -(\sqrt{T_i B}\sqrt{\frac{T_i}{T}})\left(1 + \frac{((f_i - f_c) - f)}{\frac{BT_i}{T}}\right) \tag{3.32}$$

$$X_2 = -(\sqrt{T_i B}\sqrt{\frac{T_i}{T}})\left(1 - \frac{((f_i - f_c) - f)}{\frac{BT_i}{T}}\right) \tag{3.33}$$

We can clearly see a dependency on $T_i$ and Bandwidth (B) in the integral limits and the difference in center frequencies$(f_i - f_c)$ merely shifts the spectrum.

Fig 3.10a is generated for an interference signal which is only present for $1\mu s$ over a chirp which is 25.6$\mu s$ in duration. We can infer from this figure that as time for interference$(T_i)$ becomes low, the spectrum of the down-converted interference will be poorly defined and we can clearly see peaks in the spectrum. As a comparison, we also look at the spectrum of interference which is present for a longer duration$(20\mu s)$ in this case the peaks are not very well defined but on the other hand spectrum will be very flat over all the frequency band.

As predicted from the simulations, if the transmitted narrow band CW signal is not wide-band post down conversion, we can see clearly that the peaks are very well defined. Else if the interference is wide-band post down conversion, then the interference floor will yield a raise in noise floor as predicted in the following figures
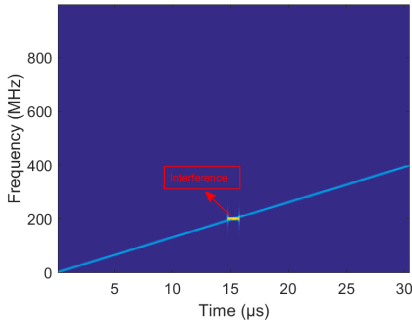


(a) spectrogram with low interference time
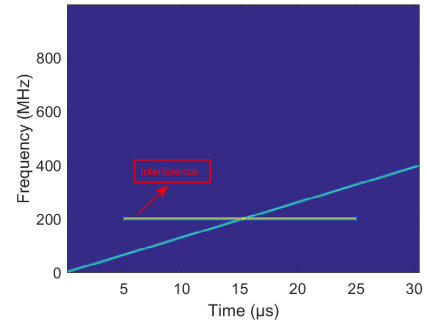
(b) spectrogram with high interference time

Figure 3.10: simulated interference spectrogram
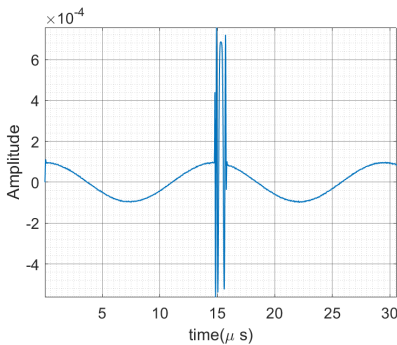


(a) time domain for low TB
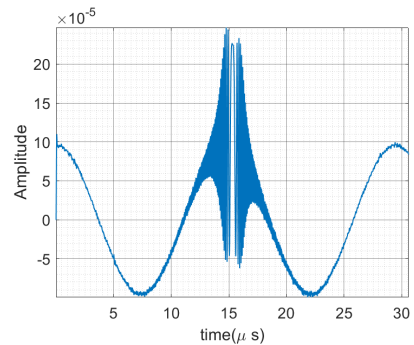
(b) time domain for high TB

Figure 3.11: simulated interference time domain

(a) frequency domain for low TB  (b) frequency domain for high TB
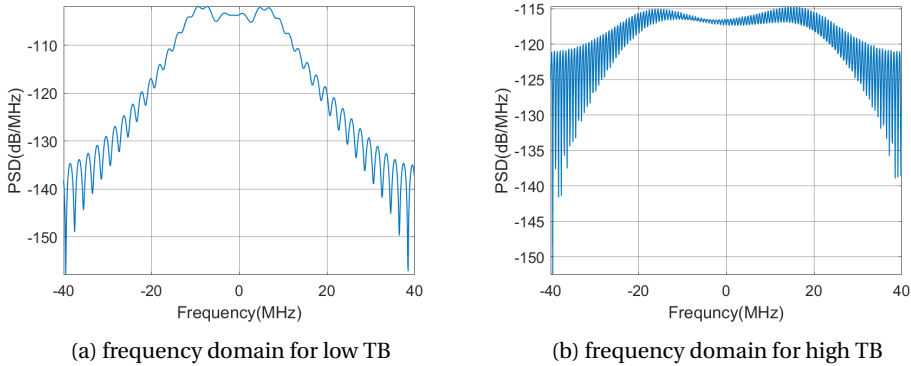
Figure 3.12: simulated interference in frequency domain post decimation

In Fig 3.10, we look at the instantaneous frequency of the transmitted signal and a simple CW interferer which is for a very short interval ($1\mu s$) and a longer interval ($20\mu s$). Subsequently in Fig 3.11, the beat signal and the time limited interference for both these cases are shown. Since we are interested to look at the interference while we are processing the signal, we look into the simulated interference scenarios post decimation, In 3.12 we look at the interference with shorter Time Bandwidth product has distinguishable peaks in its spectrum where as interference with higher TB product has increased noise floor after decimation. The additional artifacts obtained due to decimation will be explained later in this chapter. To test this scenario, we have set up an experiment with a CW interference with a transmit time of $1\mu s$ at 78.85 MHz against NXP radar working at a start frequency of 78.7 MHz with a Bandwidth of 100 MHz. Fig 3.13b shows that the noise floor increases due to the spread of interference as predicted in simulations.



(a) spectrum without interference  (b) spectrum with interference
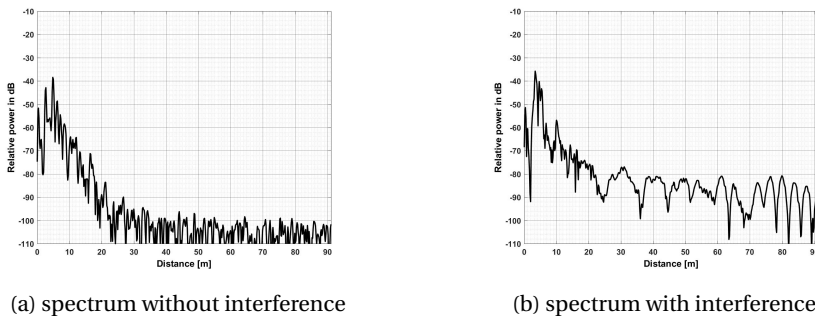
Figure 3.13: presence of interference in real data

## 3.6. INTERFERENCE IN RANGE ANGULAR DOMAIN

In our simulations, we have considered an antenna array of 12 receiver antenna elements. At a certain angle of arrival, the way that interference is superposed over these elements is predictable in angular domain but not so obvious in doppler(since the local

oscillator of interference and our radar are not synchronized). Hence we would expect
a response very similar to the response of the array pattern in angular domain. A range
angular map of interference at an angle 10° and an object at 10 m and 30° is shown in
the figure below.
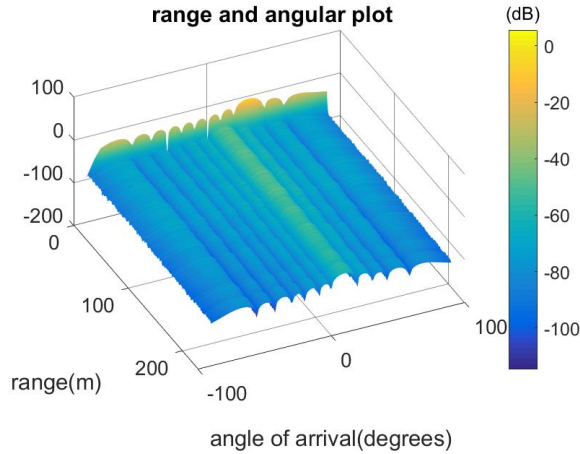


Figure 3.14: Interference in range angular domain

## 3.7. INTERFERENCE IN DOPPLER ANGULAR DOMAIN

Receiver noise will not have any particular structure in time or frequency, this is the rea-
son noise would spread over all the angle-Doppler space. Where as Interference will be
having a distinct angle of arrival but will not have any doppler localization, hence the
interference energy is same over the doppler which gives a ridge [26] this effect can be
seen in Fig 3.15.
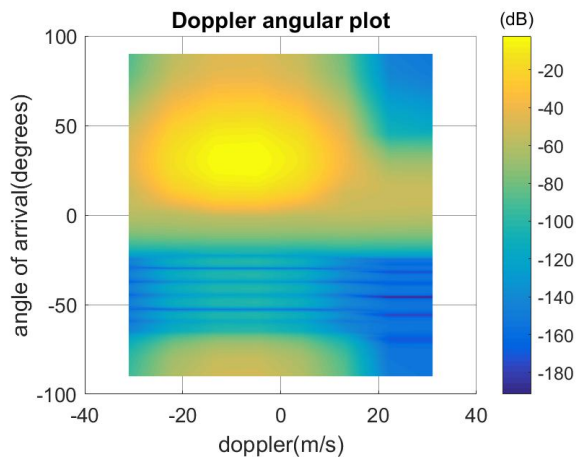


Figure 3.15: Interference at 30° and object at 30° and 20 m/s in doppler angular domain

We can see a peak which is the object at 20 m/s and at an angle 30° and an interferer is present at 10° but as mentioned in the previous section, the interference would not have synchronization over doppler, hence it is spread all over the doppler scale.

## 3.8. INFLUENCE OF LPF ON INTERFERENCE

The analog filter that we are using post mixer is very critical for understanding the wide band effect of interference. The integrated interference power is influenced by the cut off frequency of the LPF, the impulse response of the LPF also plays a very important role in estimating the number of samples interfered, this will be shown in the following sections.
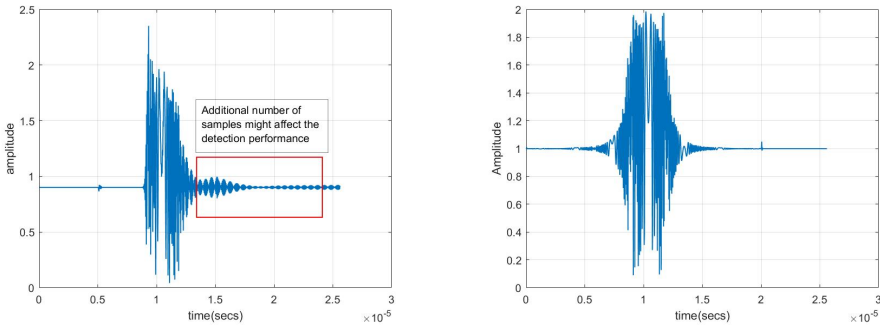


(a) absolute value of interfered beat signal under the influence of LPF with higherorder(N=30)

(b) absolute value of interfered beat signal under the influence of LPF with lower order(N=2)

Fig 3.16a shows ringing due to the higher order of the filter. This ringing would raise our threshold while applying CFAR, resulting in sub-optimal performance. In order to overcome this, we have optimized LPF to have a lower order, so that the ringing does not have an impact on the interference detection performance. Also for the equations predicting presence of interference, it is better if the interference is cut off sharply post LPF so that the number of samples and time stamp can be predicted with better accuracy. Hence we use an elliptic filter with an order 2, the ringing and sharpness is taken care of during filtering. Fig 3.16b shows the output of a lower order elliptic LPF. Both figures here are the absolute values of the complex beat signal. For our detector we are going to use absolute values of the received complex signal, so the beat signal from a single reflector scenario would have a constant amplitude when there is no interference.

It is evident that ringing would have some effect on detection performance, but the effect of ringing is still inconclusive. This topic is viable for further research. But, for our thesis, we use an analog LPF of lower order to make sure ringing does not affect our detection system. We also have a decimation filter to get the data into 40MHz for processing. Intuitively, down sampling the data might seem that the SINR will be improved. We have considered an interference which is over all the frequency band post down conversion, down sampling will only neglect the higher frequency component but interference in the pass band will still be there.

## 3.9. INTERFERENCE THROUGH THE RECEIVER CHAIN

In this section, we look at the interference at different blocks of the receiver chain and calculate the power level of interferer at each stage. For understanding this we have taken the situation where a CW interferer is present for a single chirp transmitted. The spectrogram of the transmitted and the received waveform are shown in Fig 3.17.

We have taken a FMCW transmit chirp of $400MHz$ bandwidth and a transmit time of $30.6\mu s$. A CW interferer is at distance of $1m$ with a frequency at $200MHz$ and is present for an interval from $5\mu s$ to $25\mu s$. A simulated target is present at a distance of $1m$. With these distances and parameters in table 1, we can calculate the Desired Signal power to be -79$dB$ and Undesired signal power to be -78$dB$
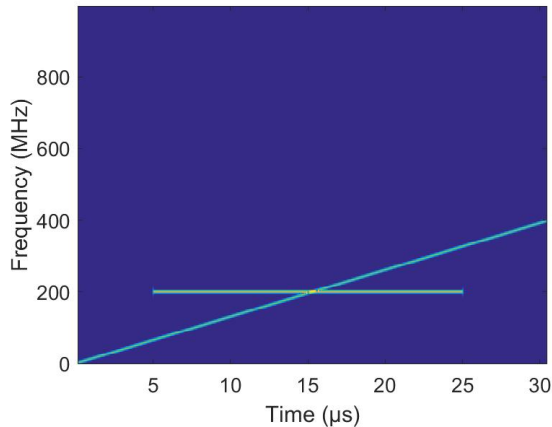


Figure 3.17: CW against FMCW for comparison

### 3.9.1. AT THE RECEIVER

At the receiver front end, the interference is expected to be present without any filtering as shown, as interference is directly superimposed over the desired signal, we would expect a raise in power level for the interval in which the presence of interference as shown in Fig 3.18. Here the interference and received reflected signal add up in linear scale giving a power level of about -72dB when interference is present, else as given the received reflected signal power level will be -79dB
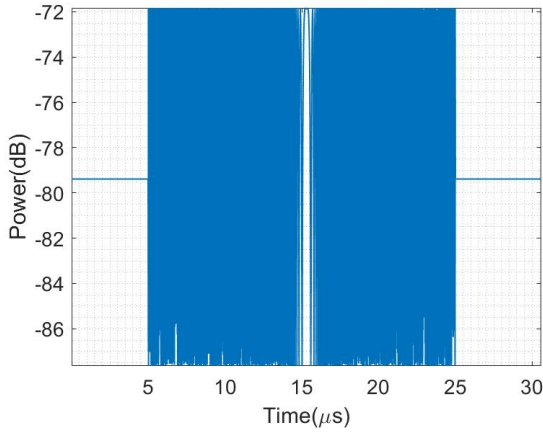
Figure 3.18: CW interferer at the receiver

### 3.9.2. AFTER THE MIXER

Now, this signal is mixed with the transmitted chirp for down conversion. Since there is nothing that affects the power level while mixing, the power level of the this received signal before and after mixing will be the same as the receiver front end
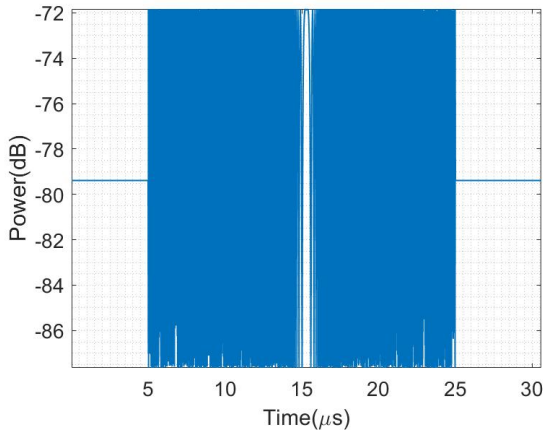


Figure 3.19: CW interferer after mixer

### 3.9.3. AFTER THE LPF

As mentioned in the previous sections, interference will be time limited by the cut off frequency of the LPF, this can be seen in Fig 3.21. Since the down converted interference has instantaneous frequency directly proportional to the time (3.21), the power level of the interference clearly would follow the magnitude response of applied second order elliptic LPF (Fig 3.20).
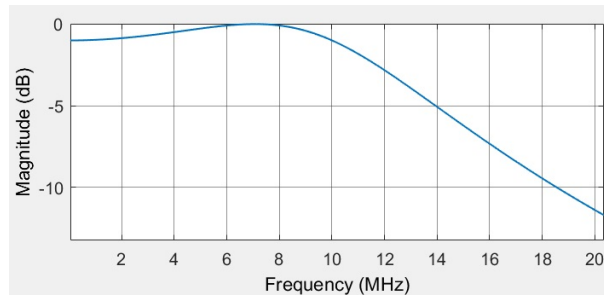
Figure 3.20: magnitude response of the LPF

Also due to the use of elliptic LPF, there would be a loss of l dB in the lower frequencies of the pass band (can be seen in the Fig 3.20). This attenuates the received reflected signal by 1 dB post LPF. The resulting power levels are shown in Fig 3.21
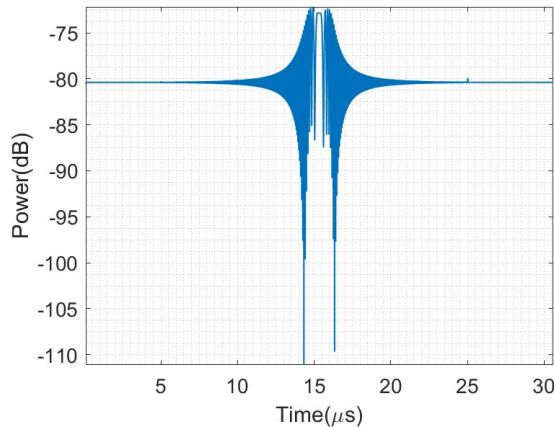


Figure 3.21: CW interferer after LPF

### 3.9.4. AFTER THE DECIMATION

Until this point in the chain, we have the analog signals, since all the simulations are done in MATLAB and considering the complexities involved in using an ADC, we have neglected the ADC use. Instead, we have decimated the low pass filtered signal directly to the sampling frequency used for processing. Decimation, being a digital down conversion at 40MHz for our case, we would have copies of our signal at regular intervals of bandwidth of 40MHz centered at [..., -40MHz,0 MHz,40MHz,80MHz,...]. But our analog LPF allows interference which has instantaneous frequency until half of the sampling frequency, which is in fact attenuated post cut off frequency. But these attenuated frequencies also enter the system and overlap with the center frequencies of the copies of the digital filter. This gives artifacts very similar to each other but attenuated due to the analog LPF. This can be observed in Fig 3.22 and can be clearly visible when we apply a

HPF which attenuates the received reflected signal in Fig 4.4b and 4.3b. The decimation for our case is done by using a simple down sampling rather than a decimation filter. It is not expected to have an effect on the amplitude of the interference post decimation with this strategy for decimation. Hence, the power level would be the same as that of after LPF.
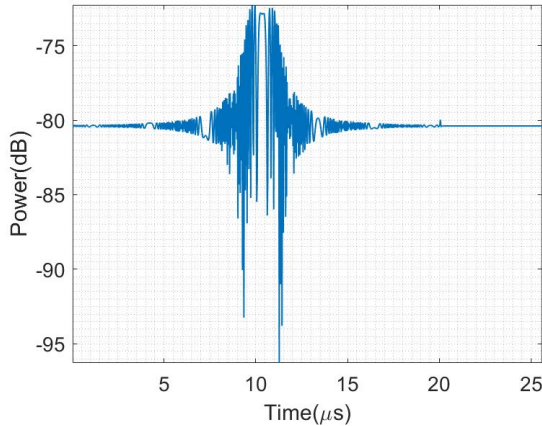


Figure 3.22: CW interferer after mixer

## 3.10. CONCLUSIONS

In this Chapter, we have seen first how the interference is localized in time domain due to the LPF. We also have looked at how the interference is unfolded in different domains and explained them with necessary equations. We tried to relate the simulation results in frequency domain to real experimental results for interference and proved why there is a raise in the noise floor in presence of interference. Finally we showed that the use of an analog LPF of a higher order will make our detection sub-optimal due to ringing and designed an optimal filter for our simulations. We also have seen how the interference unfolds in every stage of the receiver chain and looked at the power levels of the interference as well.

# 4

# DETECTION AND LOCALIZATION OF INTERFERENCE

Before doing any mitigation, we have to detect and identify the interference. In [4], insights on how to identify power levels of interferer and localize the interference over the received reflected signal are given.

We are trying to obtain information regarding the samples that are interfered for which, we have to detect the interference as early as possible in the digital domain of the receiver chain as shown Fig 1.3, hence we try to detect interference just after analog to digital conversion so that we don't loose any additional information regarding interfering samples.

If the signal and noise levels are constant, we could apply simple thresholding to detect peaks of the interferer. Then, the interference detection sensitivity would be limited by the desired signal. In reality, noise and signal levels are not constant, so we need an adaptive thresholding technique. Also, [13] mentions using CFAR filtering algorithm for detection of interference. But interference is assumed to have higher amplitude than reflected signal in most of the detection cases. In our detector, we have used a High Pass Filter(HPF) with a specific cut off to attenuate the received reflected signal and isolate the interference. We will also show that isolation of interference can be done even if the interference peak power is much lower than the reflected signal component.

## 4.1. DESCRIPTION OF THE PROBLEM

For the detection problem, We have considered a FMCW transmitted signal of 400MHz and transmit time of $30.6\mu secs$ with an object present at 1 m and FMCW interferer of the same bandwidth at 1 m but a transmit time of $5\mu s$ as shown in Fig 4.1a. As mentioned before, we are doing all the simulations in baseband, hence for FMCW case we have considered the center frequencies to be the same. Another case with similar transmitted signal but with a CW interferer at 10 m which has a center frequency of 133MHz and transmit time of about $20\mu s$ as shown in Fig 4.2a is considered. As mentioned in Chapter

1, we will consider the first 5 $\mu s$ of the transmitted signal as redundant to make sure the Phase Locked Loop(PLL) is working in linear mode. Hence, while processing, the interference will be shifted by 5 $\mu s$ in the processing stage as shown in Fig 4.2b and Fig 4.1b. The proposed detection, identification and avoidance techniques are applied in the processing stage.



(a) FMCW interference instantaneous frequency

(b) FMCW interference time domain
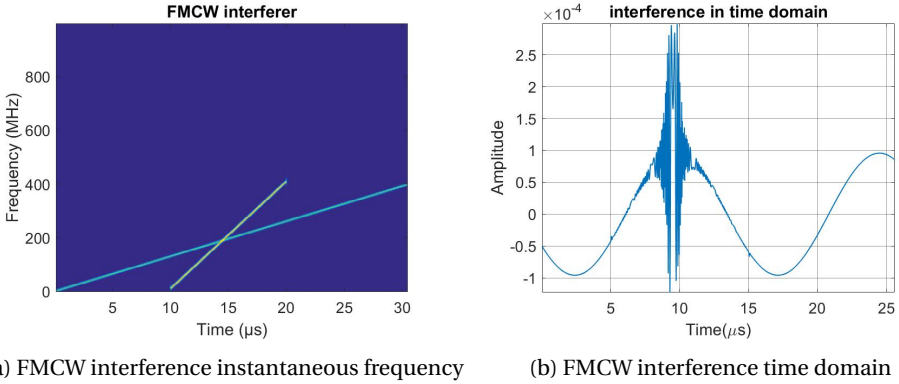
Figure 4.1: FMCW interference scenario used for the detection problem in frequency and time domain



(a) CW interference instantaneous frequency

(b) CW interference in time domain
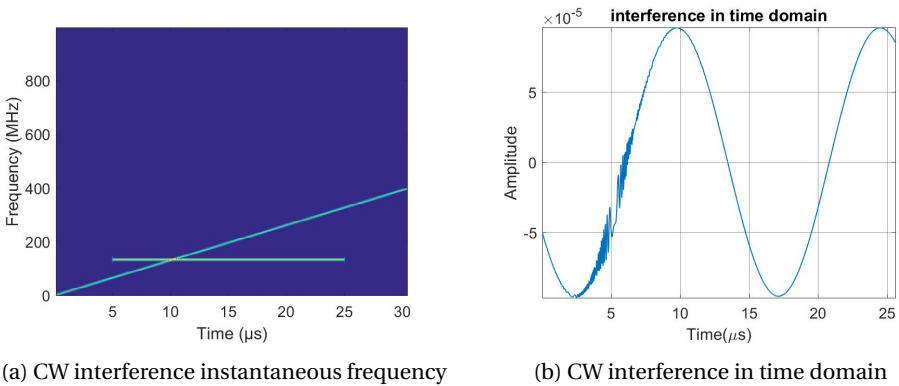
Figure 4.2: CW interference scenario used for the detection problem in frequency and time domain

Most of the existing detector/identifiers for interference detection assume that the interference power is much higher than the received reflected signal power Fig 4.1b. We have proved in chapter 3 that there will be a raise in the noise floor, even if the interferer power level in time domain is lower than the received reflected signal power level. In this case interference Power Spectral Density (PSD) might be higher than the noise PSD giving a reduced dynamic range for detection of the object. Hence our interest is also to detect interference when the interference power level is lower than the received reflected signal power as shown in Fig 4.2b. For this purpose, We propose a method using a combination of High Pass Filter(HPF) and Constant False Alarm Rate(CFAR) thresholding to detect the

presence of interference.

## 4.2. Algorithm for detection

First step of the detection is to isolate the interference from the received reflected signal component, this will be done by using a HPF. This isolated interference is to be tested with the necessary threshold to check if the interference power is higher than the specified noise level. Finally, we check if the detected $M$ samples are actually present in the window which would give actual detection, if these samples are not localized in this window then it would lead to a false alarm.

---

**Algorithm 1:** Detection algorithm for interference

1. High pass filter the received signal.

2. Estimate Noise power and calculate the threshold to be applied by CFAR.

3. Select $M$ samples with the highest power levels.

4. Check if these $M$ samples are in the preset window.

---

The flow of this algorithm will be explained in the further sections.

### 4.2.1. Use of HPF

First, we use a HPF to attenuate the received reflected signal. Since we have assumed a worst case scenario of wide band interference post down conversion, we try to isolate the interference using a High Pass Filer (HPF). This technique would work very well for interference which has flat PSD over all the frequencies. Hence, equation (3.19) can be extended to the application of HPF as

$$s_{mh} = \begin{cases} s_{mi} & \frac{-f_{LPF}+2S_2\tau_2+(f_i-f_c)}{(S_2-S_1)} \leq t \leq \frac{-f_{HPF}+2S_2\tau_2+(f_i-f_c)}{(S_2-S_1)} \\ s_{mi} & \frac{f_{HPF}+2S_2\tau_2+(f_i-f_c)}{(S_2-S_1)} \leq t \leq \frac{f_{LPF}+2S_2\tau_2+(f_i-f_c)}{(S_2-S_1)} \\ 0 & otherwise \end{cases} \tag{4.1}$$

where, $s_{mh}$ is the high pass filtered mixer signal and $s_{mi}$ is the mixer signal (3.20).
Since we intend to use a high pass filter after ADC, we have to use a digital filter. Digital filters would have a steeper cut off than analog filters. The cut off frequency of the HPF should be designed specifically to attenuate the received reflected signal component. For the design of HPF, we have considered the point where desired signal power is equal to noise power. Setting equation (3.6) to 0 and solving for the distance we get,

$$d = \sqrt[4]{\frac{P_t G_t G_r \sigma}{(4\pi)^3 \eta}} \tag{4.2}$$

and the respective beat frequency, which the cut off frequency of the HPF is given as

$$f_{HPF} = \frac{2Bd}{Tc} \tag{4.3}$$

where, $\eta$ is noise power, parameter $d$ is the distance at which desired signal power would be lower than noise power (i.e the distance after which the object is buried under the noise). The proposed method uses a cut off frequency which corresponds to the beat frequency at this distance to remove the objects and look only at interference.

## 4.2.2. INTERFERENCE POST HPF

In this section we discuss about the power levels of the interference post HPF. The applied high pass filter would attenuate the reflected signal component and also part of the interference signal. This would intuitively suggest that the integrated interference power is reduced post HPF.

With the data corresponding to the figures, we show the effect of HPF on the interference signal post decimation. Fig 4.3 and 4.4 describes using HPF to attenuate the beat signal. Using HPF also has a dis-advantage of attenuating a part of wide band down converted interference.
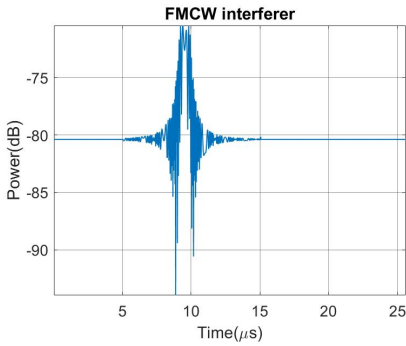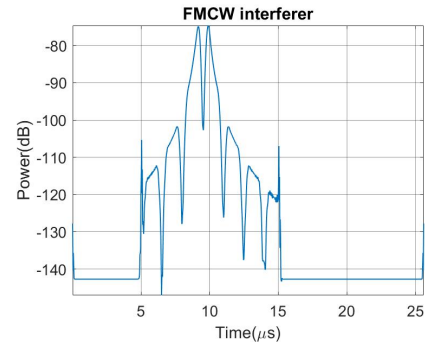


(a) FMCW interference and beat signal          (b) FMCW interference in time domain post HPF

Figure 4.3: FMCW interference scenario pre and post HPF
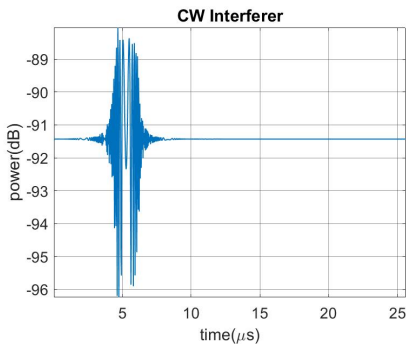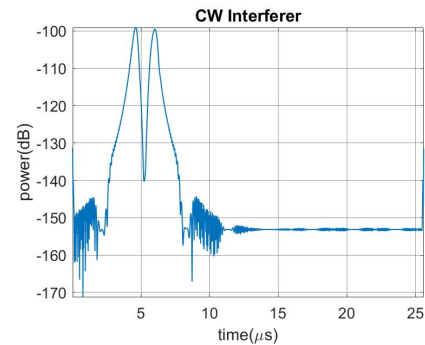


(a) CW interference and beat signal          (b) CW interference in time domain post HPF

Figure 4.4: CW interference scenario pre and post HPF

Also in the Fig 4.4b and Fig 4.3b we can observe the copies of the interference due to digital filtering. But these copies has a power of 25 dB less than the interference peak power. So we neglect samples which correspond to these copies for our detection problem. It is also quite evident that the interference can be isolated even if it has a power level much lower than that of the reflected signal component as shown in Fig 3.4, we can isolate and look at the interference post HPF until the peak power level of the interferer is higher than the noise.

### 4.2.3. Detector

For detection, we take time domain signal post HPF and check for the presence of interference. This can be formulated as a problem of detecting a deterministic signal with an unknown amplitude in presence of noise. Specifically

$$\begin{cases} H_0 : w[n] & n = l, l+1, l+2....l+m \\ H_1 : \hat{A}^2 + w[n] & n = l, l+1, l+2....l+m \end{cases} \tag{4.4}$$

Where, $H_0$ is the null hypothesis, is the interval in which we will not be able to find the interference, $H_1$ is the interval where we might find interference, $\hat{A}$ is the amplitude of interference signal, $w[n]$ is the noise, $l$ is the minimum bound of the interference signal and $m$ is the length of the interference signal. We now derive our detector specifically for our case on basis of these assumptions and necessary modifications to the detector in presence of noise given in [7].

Power of the interference signal($\hat{A}^2$) is estimated by using a square law detector. We also need to find $l$ for understanding where the interference is localized in the beat signal in time domain. This detection test would be done over each sample to detect the interference bounds from which $l$ can be found, but we assume initially that $l$ is known prior to evaluate the performance of our detector.

Since we have a complex signal for simulations we have considered complex noise, this is given as

$$w[n] = X_1[n] + i X_2[n] \tag{4.5}$$

Where $X_1$ and $X_2$ are normally distributed random variables. Since the absolute value squared of two normally distributed variables is a Rayleigh distribution and square of a Rayleigh distribution is an exponential distribution.

Our new random variable $w$ is the absolute value squared of random variable X which is a Rayleigh distribution

$$w[n] = |\sqrt{X_1^2[n] + X_2^2[n]}| \tag{4.6}$$

the PDF of $w[n]$ is a Rayleigh distribution and is given as

$$f_x(w) = \frac{|w|}{\sigma^2} \exp^{-\frac{|w|^2}{2\sigma^2}} \tag{4.7}$$

and the variance of the rayleigh distribution is given as

$$var(w) = \left(\frac{4-\pi}{2}\right)(\sigma^2) \tag{4.8}$$

the square of rayleigh distributed random variable is an exponential distribution. Let $Y = |w|^2$ is an exponentially distributed random variable the PDF of this variable is shown here, For $\sigma^2 > 0$. The transformation $Y = g(w) = |w|^2$ with inverse $w = g^{-1}(Y) = \sqrt{Y}$ and Jacobian is given as

$$\frac{d(w)}{d(Y)} = \frac{1}{2\sqrt{(Y)}} \tag{4.9}$$

therefore by using the transformation technique, we have the PDF of $Y$ as

$$f_x(Y) = f_x(g^{-1}(w))|\frac{d(w)}{d(Y)}| \tag{4.10}$$

so

$$f_x(Y) = \frac{1}{\sigma^2} \exp^{\frac{-Y}{(2\sigma^2)}} \tag{4.11}$$

Now the probability density functions of both hypothesis are given as

$$p(Y, H_1) = \frac{1}{\sigma^2} \exp^{\left(\frac{-(Y-\hat{A}^2)}{2\sigma^2}\right)} \tag{4.12}$$

is probability density function of desired target and

$$p(Y, H_0) = \frac{1}{\sigma^2} \exp^{\left(\frac{-Y}{2\sigma^2}\right)} \tag{4.13}$$

is probability density function of noise.

The theoretical probability of detection is the probability of detection of target with a threshold $T$. This is given as

$$Pd_{th} = \int_T^\infty p(Y, H_1) = \int_T^\infty \frac{1}{\sigma^2} \exp^{\left(\frac{-(Y-\hat{A}^2)}{2\sigma^2}\right)} \tag{4.14}$$

giving us the theoretical estimated probability of detection as

$$Pd_{th} = 2\left(\exp^{\left(\frac{-T+\hat{A}^2}{2\sigma^2}\right)}\right) \tag{4.15}$$

SETTING THE THRESHOLD

Taking likely hood ratio for all the samples in the window $m$, we get

$$L(Y) = \frac{\prod_{n=1}^m p(Y; H_1)}{\prod_{n=1}^m p(Y; H_0)} \underset{H_0}{\overset{H_1}{\gtrless}} \gamma \tag{4.16}$$

substituting the pdf's (4.13) and (4.12) in the above equation,

$$L(Y) = \frac{\prod_{n=1}^m \frac{1}{\sigma^2} \exp^{\left(\frac{-(Y-\hat{A}^2)}{2\sigma^2}\right)}}{\prod_{n=1}^m \frac{1}{\sigma^2} \exp^{\left(\frac{-Y}{2\sigma^2}\right)}} \underset{H_0}{\overset{H_1}{\gtrless}} \gamma \tag{4.17}$$

and solving further, we get the log likely hood ratio as

$$h(Y) = \log(L(Y)) = \left( \sum_{n=1}^{m}(Y) - \sum_{n=1}^{m}(Y - \hat{A}^2) \right) \underset{H_0}{\overset{H_1}{\gtrless}} \gamma^1 \qquad (4.18)$$

where $\gamma^1 = \log(2\sigma^2\gamma)$ is the updated threshold. Now let us detect only 1 sample with a sample number $m$, then as an example, the log likely-hood ratio is

$$h(Y) = \left( \hat{A}^2 \right) \underset{H_0}{\overset{H_1}{\gtrless}} \gamma^1 \qquad (4.19)$$

in this equation $\hat{A}^2$ is the power of interferer, so it means power of the interfering sample needs to be estimated and for that we have used a peak detector (for a single interfering sample). so the comparison of $h(Y)$ becomes

$$\hat{A}^2(n = m) \underset{H_0}{\overset{H_1}{\gtrless}} 2\sigma^2\gamma^1 \qquad (4.20)$$

where $\hat{A}$ is the estimate of amplitude of interfering sample and

$$T = 2\sigma^2\gamma^1 \qquad (4.21)$$

is the threshold. So the performance of detector would be directly dependent on the estimate of power of the interfering sample $\hat{A}^2$. In order to make this decision, we need to set the threshold accordingly, but the aforementioned equations are in practice for a constant noise level. In reality, noise levels are often variable and has to be estimated from the signal itself. Hence, the noise power is to estimated from the samples surrounding our cell under test and set the threshold accordingly. For this estimation of threshold, we use CFAR techniques.

Cell Averaging(CA) CFAR is based on an assumption that targets(peaks) are isolated and separated by at least the reference window. Fig 3.19 shows that the interference consists of peaks closely spaced to each other. This would lead us to apply extended CA-CFAR techniques. Considering Greater of Cell Averaging (GOCA) CFAR, it misses the detection of peaks near the clutter edges due to elevated masking effect. Due to computational complexity Ordered Statistics(OS) CFAR is not used in detection. Considering the above limitations for various CFAR techniques, a Smallest of Cell Averaging(SOCA) CFAR is used for detection of the interference on the beat signal[26]. In SOCA, lead and lag windows are averaged separately to two independent estimates of the background. The threshold is computed by the two estimates of the signal+noise power level in two windows as shown below

$$\beta_1^2 = \frac{1}{K} \sum_{i=1-K}^{1} |x_i|^2 \qquad (4.22)$$

$$\beta_2^2 = \frac{1}{K} \sum_{i=1}^{K} |x_i|^2 \qquad (4.23)$$

where, $K$ is the window size that used for SOCA CFAR. Now the threshold for SOCA is given as

$$T = \alpha_S \min(\beta_1^2, \beta_2^2) \qquad (4.24)$$

where, $\alpha_S$ is the multiplication factor. The threshold must be calculated iteratively from the given $P_{FA}$. For this we ideally should calculate the multiplication factor $\alpha_S$ and then replace it in the equation for threshold(4.24). To calculate $\alpha_S$, we have to set a particular false alarm rate $P_{FA}$ as shown below.

$$\hat{P}_{FA/2} = (2 + \frac{\alpha_S}{(K/2)})^{-K/2} \sum_{i=0}^{K/2-1} \binom{\frac{K}{2}-1+i}{i} \left(2 + \frac{\alpha_S}{(K/2)}\right)^{-i} \tag{4.25}$$

From these set of equations we calculate $P_d$ and threshold values. For our detector, we have used a typical $P_{FA} = 10^{-6}$ and the threshold values are calculated from (4.24). This threshold will be substituted in (4.20) to make the decision for desired detection.

### 4.2.4. MAXIMUM NUMBER OF INTERFERING SAMPLES

For applying our detector, we have to know the maximum probable interfering samples for multiple sample detection to analyze the performance of our detector and understand the limitation on the number of interference samples that can be detected. It was shown in Chapter 3 that interference can be localized into a certain window depending on slope of interferer and cut off of the Low Pass Filter in (3.19). It is assumed that slope of interferer and slope of transmitted signal $S_2$ and $S_1$ are known prior to the application of detector. In later sections, we also show a way to estimate the slope of the interferer but for now it is assumed to be known. We use this information to understand the limitation on the number of samples that can be detected and analyze the performance of the detector in these cases.

The number of interfering samples can be calculated from (3.18) as given in [4]

$$M_{int} = T_{inter}f_s = \frac{2f_s f_{LPF}}{S_2 - S_1} \tag{4.26}$$

The number of interfering samples is dependent on low pass filter cut off frequency. This also suggests that the designing of LPF is very critical for detecting the interference accurately.

**Example 4.2.1.** Calculate number of interference samples for CW interference with the $S1 = 400\text{MHz}/(30.6\mu s)$, $f_{LPF}$=10MHz and $f_s$ is 40MHz.

1. Since it is a CW interferer, S2=0

2. Substituting the values in (4.26) , we get $M_{int} = 60$samples

**Example 4.2.2.** Calculate number of interference samples for FMCW interference with a slope of $S2 = 400\text{MHz}/(10\mu s)$ with the $S1 = 400\text{MHz}/(30.6\mu s)$, $f_{LPF}$=10MHz and $f_s$ is 40MHz.

1. Substituting the values in (4.26) , we get $M_{int} = 30$samples

## 4.3. PERFORMANCE OF THE DETECTOR

To analyze the performance of our detector, we are going to look at the performance of detector in detecting single and multiple samples of interferer. We have set up a simulation with Interference to Noise Ratio(INR) ranging from 0 dB to 40 dB for four cases namely,

- Signal + interference: where the detector is applied only on the received signal component.

- Signal + interference with HPF: where the detector is applied on the received signal component post HPF.

- Interference only: where the detector is applied on the simulated interference component.

- Interference post HPF: where the detector is applied on the simulated interference component post HPF.

With the help of $10^4$ Monte-Carlo simulations , we calculate the probability of detection for all these cases. We compare this probability of detection with its theoretical estimate (4.15).

### 4.3.1. DETECTION OF A SINGLE SAMPLE

Detector performance while detecting a single interference sample is shown in Fig 4.5a for a FMCW interferer and Fig 4.5b for a CW interferer .



(a) detection of 1 sample FMCW interferer    (b) detection of 1 sample for CW interferer
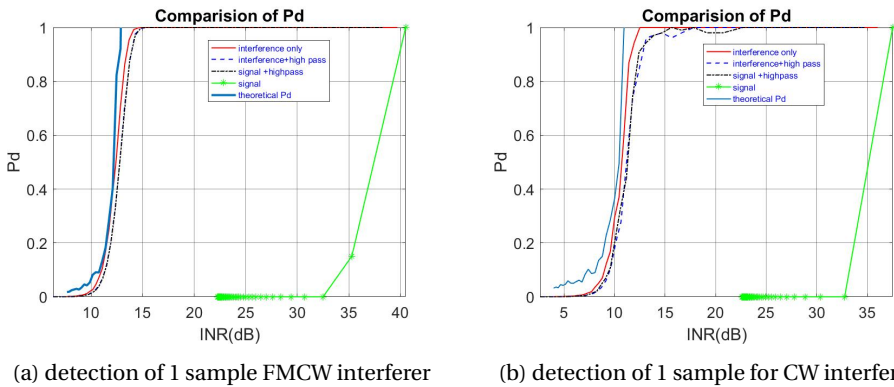
Figure 4.5: Performance of proposed detector for single interference sample detection

The use of a High Pass filter for interference detection has a significant improvement on performance of detector. In theory, we have considered the interference to be having constant power over its duration, post HPF the power of interference is not constant (as there will be some attenuation due to HPF), so there will be a deviation of about 0.5 dB from the theoretically predicted value. There is a gain of about 15 dB while using a HPF for detection as can be seen in Fig 4.5. This gain is due to HPF will be discussed later in this section.

We have considered a $2^{nd}$ order analog LPF with a cut off frequency of 10MHz and a $20^{th}$ order digital High Pass filter with a cut off 6MHz for this case, the compound effect would give an attenuation of about 0.6 dB while estimating the power of interferer. This can be clearly seen in Fig 4.6 which shows a loss of about 0.6 dB at the point where frequencies of analog low pass and digital high pass are equal. The instantaneous frequency of

interference post down conversion is linearly dependent with time (3.16), interference
samples also have a frequency which is proportional to time. Hence when we apply a
high pass filter over these samples, we can see that the distribution of samples over time
domain is very similar to magnitude response of our filters. This would mean that the
power levels of these interfering samples would be proportional to the magnitude re-
sponse of the applied compound filter. Since this compound filtering effect has 0.6 dB
as peak magnitude, this would directly reflect on our detector as can be seen in Fig 4.5b
and Fig 4.5a. Hence, it can be concluded that the detector performance would depend
on the estimated power level of interference sample (4.19) which in turn would depend
on the magnitude response of compound filtering.
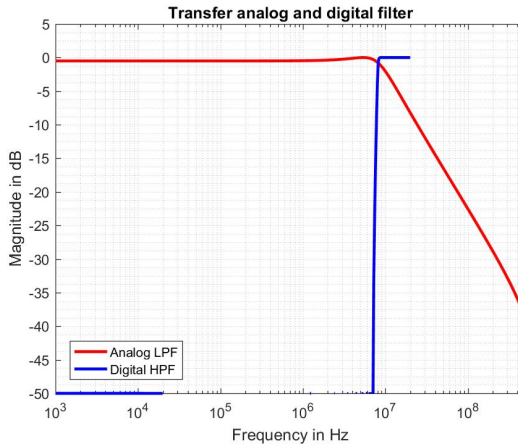


Figure 4.6: loss of dB due to combined filtering

## 4.3.2. DETECTION OF MULTIPLE SAMPLES

Since we have used a high pass filter, the number of interfering samples is reduced by a
factor proportional to the difference of cut off frequency of HPF and the cut off frequency
of LPF. Thus, the number of samples that can actually be detected in the presence of HPF
is given as

$$N_{int} = \frac{2f_s(f_{LPF} - f_{HPF})}{S_2 - S_1} \tag{4.27}$$

so the maximum number of samples that can be detected for FMCW interferer case in
presence of HPF is for the test case 4.2.2

$$N_{int} = \frac{2f_s(f_{LPF} - f_{HPF})}{S_2 - S_1} = 12$$

Fig 4.7b shows detection probability of 10 interfering samples.
Similarly, the number of interfering samples for CW interferer in test case 4.2.1 case in
presence of HPF is given as

$$N_{int} = \frac{2f_s(f_{LPF} - f_{HPF})}{S_2 - S_1} = 24$$

(a) detection of 10 samples in 12 possible interference samples for FMCW case

(b) detection of 10 samples in 24 possible interference samples for CW case
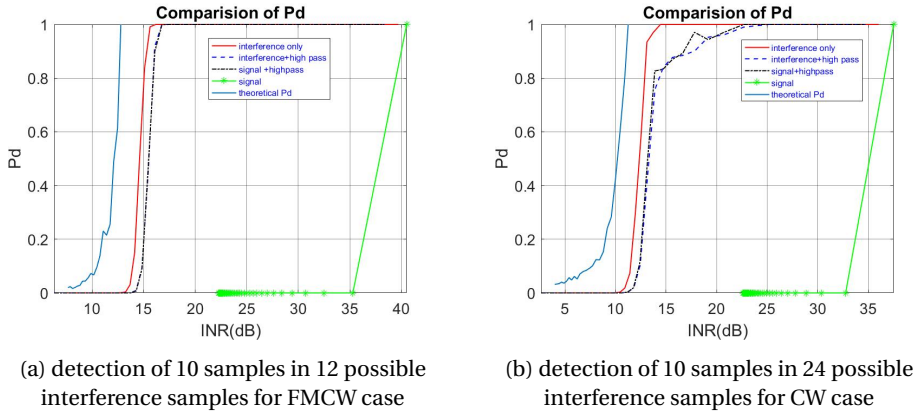
Figure 4.7: Performance of the proposed detector for multiple interference samples detection

The loss that accounts for multiple samples detection can be explained from Fig 4.8a. When there is no HPF applied, threshold tends to be much higher than signal plus interference level because of the presence of received reflected signal component. Post HPF, we can have a clear estimate of the interference power from the previous sections for a single sample detection. While on the other hand, not all the interference samples have same power levels post HPF. Post HPF, signal might not contain the required number of samples above the applied threshold. This is why we observe a loss of about 3dB from theoretical estimate while detecting multiple samples.



(a) effect of high pass on the signal and threshold

(b) samples detected post HPF
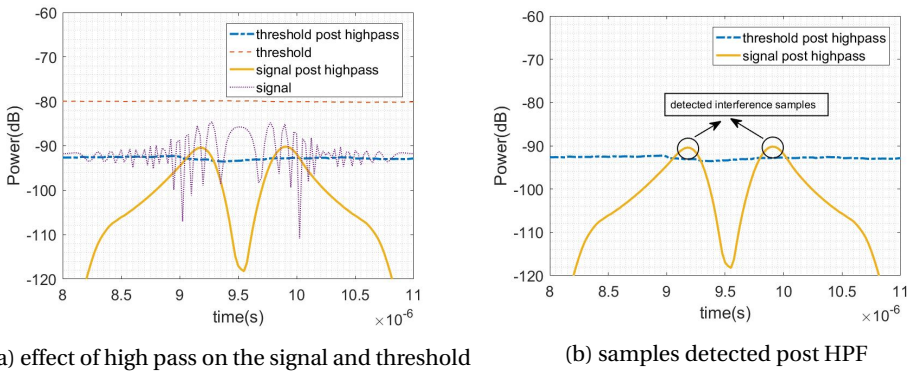
Figure 4.8: Performance of the proposed detector for multiple interference samples detection

## 4.4. MITIGATION BY NULLING

In this section we look at a simple mitigation technique proposed by [16]. The idea is to null the interfering samples. We have shown a way to detect the interfering samples by using a HPF and CFAR thresholding. These interfered samples' amplitude is set to 0 for this mitigation technique and the results are as shown below.

(a) time domain nulling of interference    (b) nulling in frequency domain
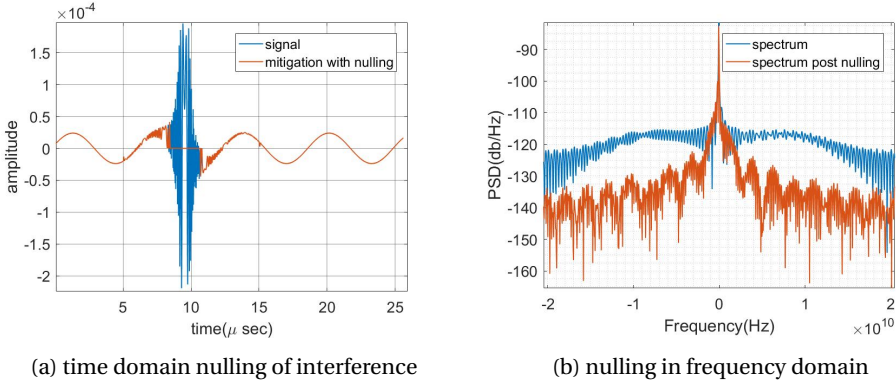
Figure 4.9: Mitigation of interference by nulling

There is an improvement of 15 dB in the Signal to Interference Ratio(SIR) due to nulling interfering samples, but the main lobe which consists of information regarding object is broadened as shown in Fig 4.9b

The disadvantages of nulling the interfering samples is spectral broadening and also typically shoulders will be appearing around the main lobe. Since we are nulling out the interference samples, the integration gain will be reduced to

$$G_I = 10\log_{10}\left(\frac{(T - T_i)^2 f_{samp}}{T}\right)$$

as mentioned in [4] and also due to nulling additional artifacts involving sinc functions will be present in the frequency domain. This is the reason why other methods such as forward prediction methods are preferred in time domain [16]. In the following sections, we also present a novel time domain mitigation technique which preserves the resolution in spectrum but removes interference completely.

## 4.5. Conclusions

To detect the presence of an uncorrelated interference, we have considered a case where we know the slope of interferer before hand. It was shown that detection of interference will be very much dependent on cut off frequency of LPF. Also, the LPF has to be designed such that group delay performance and order of the filter does affect the performance of our detector. The cut off of the high pass filter used for isolation of interference plays a very critical role in detection performance, this HPF cut off frequency should be calculated in a way that the reflected signal is attenuated. Otherwise the un-attenuated reflected signal will affect the performance of our detector by setting the threshold higher. The performance of detector in a CW interferer is slightly better than that in a FMCW interferer case. In a CW interferer, with the given transmit power, we will be able to detect an interference sample with a probability of at least 0.8 if the sample has a power level of 12 dB. Where as in the presence of FMCW interferer, with the given transmit power, we will be able to detect an interference sample with a probability of at least 0.8 if the

sample has a power level of 15 dB. We also have proved that there is a limit in number of interferer samples post HPF that can be detected in section 4.3.2.

For detecting multiple samples, in a CW interferer for detecting 30% of samples, the INR should be at least 14 dB to detect these samples with a probability 0.8. For detecting multiple samples, in a FMCW interferer for detecting 20% of samples, the INR should be 16 dB to detect these samples with a probability of 0.8.

This is due to the presence of higher number of samples in CW interferer case than in FMCW interferer case. So it also intuitively suggests that this detector needs higher number of interfering samples for a better detection. Due to the compound filtering effect, we will be having a loss of 0.6 dB on the power level of the interferer and hence there will be a deviation.

The performance of detector drops by 3dB when multiple samples are to be detected because higher integrated interference power is required to detect multiple samples.

In the next section we look at a simple mitigation technique using nulling to mitigate interference from received signal and have seen a reduction in the noise floor. Also, we observed a dis-advantage of losing the information regarding the beat signal and also we would observe a raise in side lobe level.

**4**

# 5

# IDENTIFICATION AND AVOIDANCE

In this section we estimate the slope and identify interference. We also propose a novel avoidance technique by estimating the bandwidth of the interferer. It was suggested in 4.2.4 that windowing over the interference is essential for a better performance of our detector. This slope estimate can be used in calculating the accurate window size over which our detector has be placed. The final piece of information that can be obtained from interfering samples is the center of the interferer and the bandwidth of interferer itself.

Let us reconsider the equations for interference and received signal with (3.10) and (3.11) with center frequency for transmission for a single chirp.

$$s_i = A_i \exp\left(2\pi j (f_i t + \frac{S_2}{2}(t - \tau_2)^2)\right) \tag{5.1}$$

Where $f_i$ is the center frequency for the interference. Similarly transmitted signal is

$$s_t = \exp\left(2\pi j (f_c t + \frac{S_1}{2}(t)^2)\right) \tag{5.2}$$

Where $f_c$ is the center frequency of transmitted signal

Post mixing with interference signal, we have an additional term pertaining to the difference of transmitted and interference center frequency,

$$s_{mi} = A_i \exp\left(\pi j ((S_2 - S_1) t^2 + S_2 \tau_2^2 - 2 S_2 t \tau_2 - 2 f_i \tau_2 - 2(f_i - f_c) t)\right) \tag{5.3}$$

The interference center is the time instant where the down converted frequency is minimum. Phase will be minimum at the time where instantaneous frequency of interference equals instantaneous frequency of transmitted signal. We find the center of the interference by differentiating the phase and equating to zero,

$$\frac{d\phi}{dt} = 2(f_c - f_i) + 2(S_2 - S_1) t - 2 S_2 \tau_2 = 0 \tag{5.4}$$

where $\phi$ is the phase of the mixer interference signal $s_{mi}$, by solving this equation we get,

$$t_{center} = \frac{S_2 \tau_2}{(S_2 - S_1)} - \frac{f_c - f_i}{(S_2 - S_1)} \tag{5.5}$$

For finding the accurate center for the interference, (5.5) has to be used. For a CW interferer since the time delay $\tau_2 = 0$, $t_{center}$ will be dependent only on the center frequency of the interferer, in this case $f_i$ can be easily predicted from the above equation as

$$t_{center} = \frac{f_c - f_i}{S_1} \tag{5.6}$$

In reality slope, time delay and center frequency of the interferer are not known and cannot be estimated just with the given information. Hence, we try to analytically find the interference center from the detected interference samples.

We have seen in section 4.3.2 that the number of samples detected has an inverse relationship with slope of interference. Up until now, we have been estimating the number of samples. But, for estimating the slope itself, we have to consider the fact that, for the same number of samples detected, we can have two possible interference signals. Hence the equation 4.26 has to be corrected to

$$M_{int} = \frac{2 f_s f_{LPF}}{|S_2 - S_1|} \tag{5.7}$$

There could be two equivalent solutions giving the same number of interference samples detected,

$$\hat{S}_{21} = S_1 + \frac{2 f_{LPF} f_{samp}}{N_{int}} \tag{5.8}$$

and

$$\hat{S}_{22} = S_1 - \frac{2 f_{LPF} f_{samp}}{N_{int}} \tag{5.9}$$

If we are able to estimate the slope of interferer over multiple ramps then it might be possible to reconstruct the interference. With this information, we can predict the frequency by which we need to hop so that we avoid the interference completely. For this technique to work we also need to accurately estimate the center of interferer, this is shown in the next section.

## 5.1. FINDING THE CENTER OF THE INTERFERER

The true value of the center is the time instant where the instantaneous frequency of interference is equal to the instantaneous frequency of the transmitted signal. We can find the center of interference by taking the derivative of received signal as explained in [27]. But this method of estimation will work only when the down converted interference is narrow band as shown in Fig 5.1. For our case, since we have considered a wide band interference post down conversion, we will have copies of the interference as described in section 4.2.2. So, the equations considering phase centers of the interference is not particularly useful as each copy will have its own phase center. In this case, we propose a simple way to estimate the center of interferer in this chapter.

Equating the instantaneous frequency components from (3.8) and (3.11) and solving for $t_{center}$, we get

$$t_{center} = \frac{f_c - f_i + S_2\tau_2}{S_2 - S_1} \tag{5.10}$$

In this section we look at finding the center of the interferer analytically. Initially we consider a single interferer case and estimate the center by looking at the received signal.
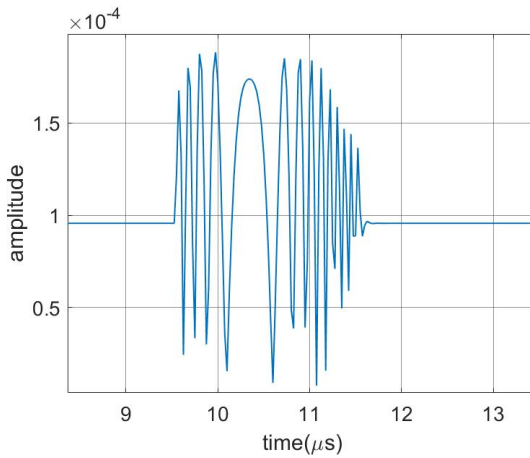


Figure 5.1: finding the center for interferer by using [27]

### 5.1.1. FINDING THE CENTER

A simpler way is to first analytically estimate the time stamps for the start and stop of the estimated interference signal from our detector and correlate the interference over the received reflected signal. The peak would correspond to the center of interferer. Equation for the correlation is given as

$$s_{corr}(n) = \sum_{m=0}^{M-1} s^*(m)\hat{s}_i(m+n) \tag{5.11}$$

where $s_{corr}(n)$ is the correlation, $s$ is the total received signal and $\hat{s}_i$ is the estimated interference component.

---

**Algorithm 2:** Finding the center

1. Detect the $M$ interference samples using a HPF.

2. Post-detection, find the limits of the time limits interferer $[M_1, M_2]$.

3. From these parameters localize the interference over the beat signal.

4. Correlate the estimated interference over the beat signal using equation (5.11) to get $s_{corr}(n)$.

5. Find the delay $n$ at which there is a maximum.

---

An example of the working of the algorithm 2 with interferer parameters given in example 4.2.2, is shown in here. First, the down converted signal is shown in Fig 5.2a. We apply our detection algorithm to find the interference in 5.2b. With this detected interference signal, we cross correlate it with the received reflected signal to find the center as shown in Fig 5.3. We clearly see that the center of the interference is at about $9.5\mu s$ in this case.



(a) received signal with interference

(b) Detected interference
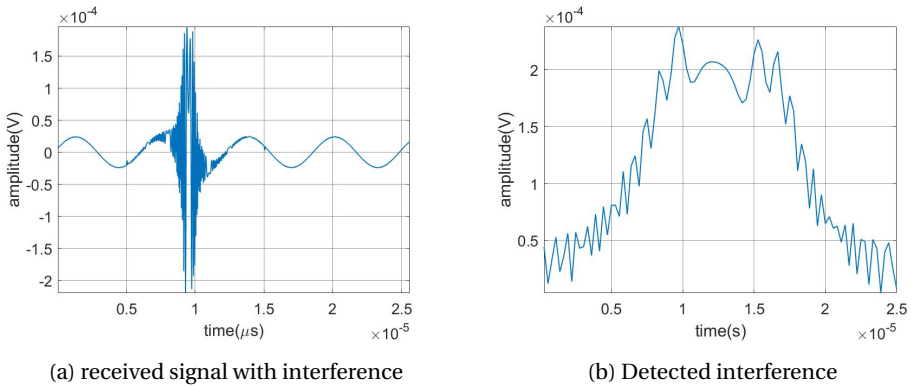
Figure 5.2: Estimation of center of the interferer
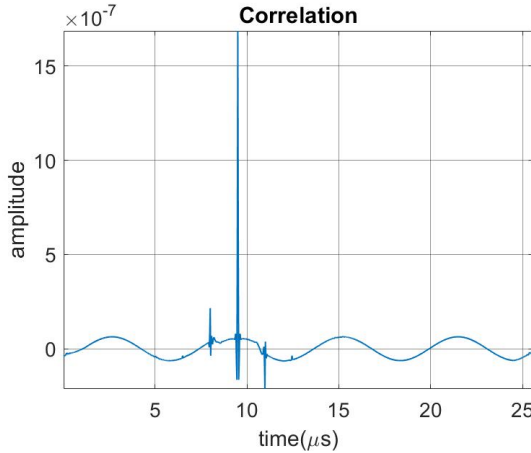
Figure 5.3: Correlation of interference and received signal

Since, the time stamps of the start and stop of the interferer are known over each ramp, we could also find the center of the interferer by just taking mid point of these two time stamps. The accuracy of this method of estimation is suggested for further research.

## 5.2. ALGORITHM FOR AVOIDANCE

Since we know the slope of the interferer and a point on the interferer, we can reconstruct this interference completely. The only unknown at this point is the bandwidth of interferer. In this section we present an avoidance algorithm which gives information about the bandwidth of the interferer and the frequency shift to avoid interference completely. Results of this algorithm are shown as follows.

### 5.2.1. DEPICTION OF ALGORITHM

For each ramp under the influence of interference, we detect the $M$ interfering samples, estimate slope and estimate the $t_{center}$. After this we reconstruct the two possible instantaneous frequencies with each $t_{center}$. When there is a change in estimated slope, we reconstruct the interferer with the information pertaining to the previously estimated slope and current slope. With this, we can predict the bandwidth of the interferer. For first ramp under the influence of interferer and center of the interferer $t_1$, the two instantaneous frequencies with the estimated slope are given as

$$\hat{f}_{int_1} = \hat{S}_{21}\, t + (\hat{S}_{21} - S_1)\, t_1 \tag{5.12}$$

$$\hat{f}_{int_2} = \hat{S}_{22}\, t + (\hat{S}_{22} - S_1)\, t_1 \tag{5.13}$$

for the next ramp under influence of interferer and center of the interferer $t_2$

$$\hat{f}_{int_3} = \hat{S}_{31}\, t + (\hat{S}_{31} - S_1)\, t_2 \tag{5.14}$$

$$\hat{f}_{int_4} = \hat{S}_{32}\, t + (\hat{S}_{32} - S_1)\, t_2 \tag{5.15}$$

---

**Algorithm 3:** Avoidance algorithm for interference

---

1. Detect M samples that are being interfered by the proposed detector as shown in section 4.2.3.

2. Estimate the slope of Interferer. $\hat{S}_{21}$ and $\hat{S}_{22}$ from (5.8) and (5.9) respectively.

3. Estimate center of interferer $t_{center}$ by using (5.11).

4. Construct two lines which give instantaneous frequency of interferer $\hat{f}_{int_1} = \hat{S}_{21} t + (\hat{S}_{21} - S_1) t_{center}$ and $\hat{f}_{int_2} = \hat{S}_{22} t + (\hat{S}_{22} - S_1) t_{center}$.

5. Repeat this over all the ramps

6. Find all the intersection points after extrapolation for the concurrent ramps if the slopes are different (a maximum of 4 points will be present).

7. Extrapolate the interference and find the point ($t_{max}$) which has the least deviation from the previous and present intersection point.

8. Estimate the shift $\hat{S}_{21} t_{max}$ of the interferer with this information.

9. Hop by a frequency corresponding to the shift frequency, $\hat{S}_{21} t_{max}$ to avoid the interferer completely.

---

By solving these linear equations, we can find the intersection points for these linear equations. Since we already have the interference intersection points (interference centers) for each ramp, we will have to predict the intersection point which is the closest to both the interference centers under test. The frequency corresponding to this point will give the information about the frequency shift to avoid the interferer.

We have considered a worst case scenario of an interferer having two different slopes for up chirp and down chirp. Since we are extrapolating the interferer when there is a change of slope, this would also work for other modulations. Let us consider $t_{max}$ as the extrapolated intersection point and estimate the instantaneous frequency of interferer corresponding to this point ,

$$f_{shift} = \hat{S} t_{max}. \tag{5.16}$$

where, $f_{shift}$ is the frequency to be shifted to avoid the interferer, $\hat{S}$ is one of the two estimated slopes of the interferer. This is the bandwidth of the interferer, if the interferer has a constant transmission bandwidth for all the interference chirps and has the same center frequency as the transmitted chirp.

## 5.3. RESULTS FOR THE AVOIDANCE TECHNIQUE

For testing aforementioned algorithm, we have considered a test case with the transmit frequency of 400MHz and a transmit time of $30\mu s$.

### 5.3.1. AVOIDING FMCW INTERFERER

#### TRIANGULAR MODULATION

An interfering signal is considered with a bandwidth of 300MHz, an upchirp time of $60\mu s$ and down chirp time of $20\mu s$ as shown in Fig 5.4 and a difference in center frequency of transmission of 10 MHz.
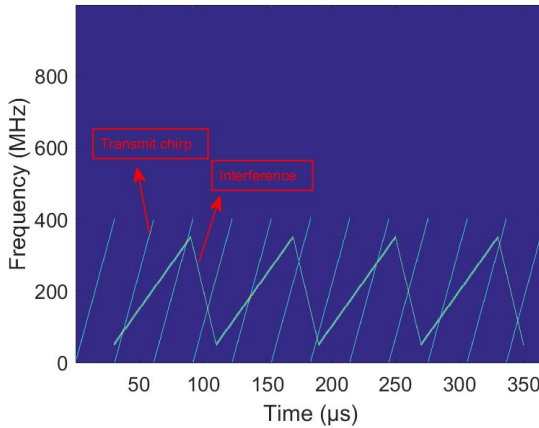


Figure 5.4: Generated transmitted and interference waveforms



(a) interference intersection points



(b) extrapolated intersection points
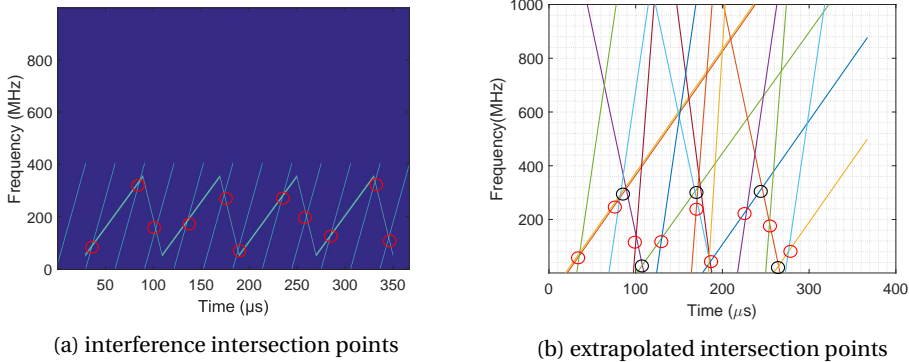
Figure 5.5: Working of algorithm

With algorithm 3, we have reconstructed the instantaneous frequency of all concurrent interfering ramps. All the intersection points are shown in Fig 5.5. Red circles represents the centers of the interference and Black circles represent the intersection points of the extrapolated instantaneous frequencies.

With this information, we shift the center frequency by the frequency corresponding to the extrapolated point (black circle). In this case it is about 310MHz. Post avoidance, the resultant transmitted wave form avoids the interferer completely as shown in the Fig 5.6.
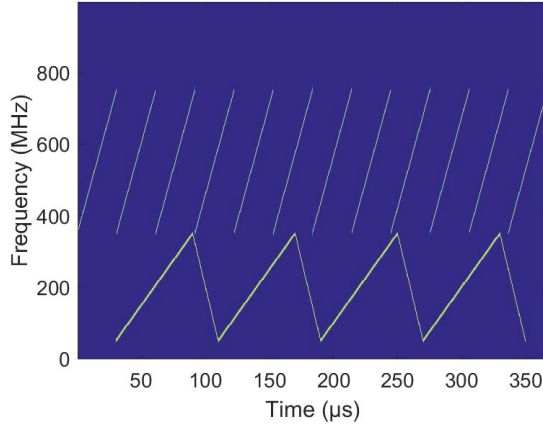
Figure 5.6: Generated transmitted and interference waveforms after applying the proposed algorithm

### SAWTOOTH MODULATION

In a more realistic scenario where the interferer is also a sawtooth modulation, the results of the avoidance technique is shown in following figures. The transmitted signal has a bandwidth of 500 MHz and a transmit time of 30.6 $\mu s$. Interferer has a bandwidth of 400 MHz and a transmit time of 90 $\mu s$ with a difference in center frequency of 100 MHz.
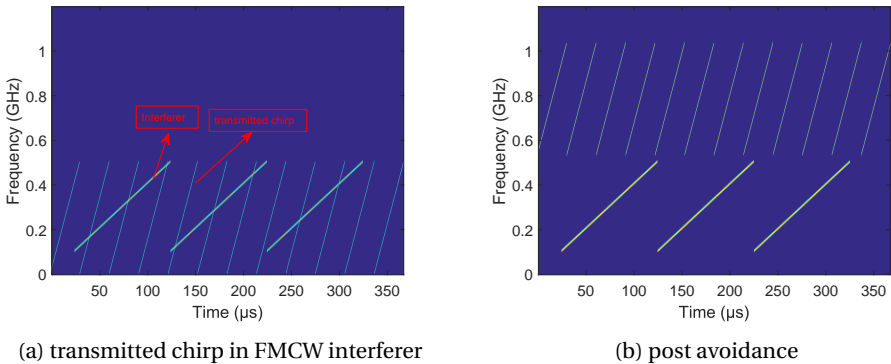


(a) transmitted chirp in FMCW interferer                    (b) post avoidance

Figure 5.7: Working of algorithm in FMCW sawtooth modulated interference

With the equations, we estimate the frequency shift to avoid the interference to be at 520 MHz. We can see that by shifting the center frequency to this value, we can avoid the interferer completely.

## 5.3.2. AVOIDING CW INTERFERENCE

To test Algorithm 3, we set up a simulation with a CW interferer at 100MHz center frequency.

(a) transmitted chirp in CW interferer        (b) post avoidance
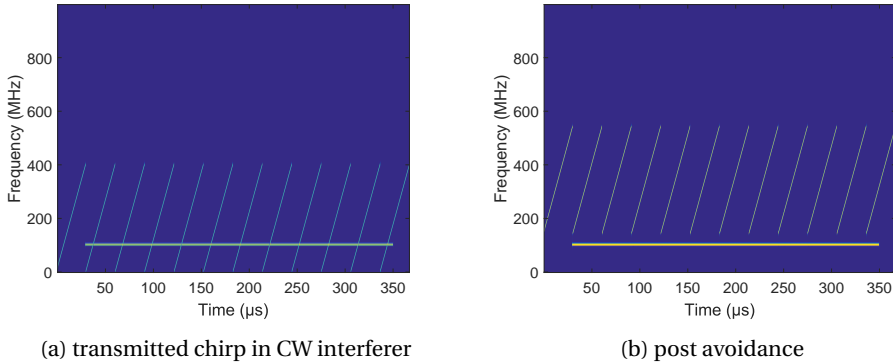
Figure 5.8: Working of algorithm in CW interference

With the proposed algorithm, we have estimated the center frequency of the CW inter-ferer to be 104MHz and shifted our center frequency by that much to avoid the interferer completely. Hence by using this algorithm, we proved that we will be able to avoid the interferer completely.

## 5.4. CONCLUSIONS

In this chapter, we have first looked at estimating the center of the interferer by using the detected interference samples, we have described a way to estimate the center of inter-ferer by using cross correlation with necessary equations. With this information, we esti-mated the bandwidth of the interferer. We proposed an algorithm to avoid interference by strategically shifting the center frequency above the interferer. To demonstrate the algorithm, we have implemented it on FMCW and CW interference and have shown that these interference can be avoided completely. The algorithm mentioned in [23] would in principle shift the frequency according to the detected interference samples. But if the interference is present in the shifted band also, then the algorithm needs to detect interference once again and shift. This makes this algorithm less efficient.

With the proposed algorithm, we estimate the shift to avoid the interferer in one-shot. The numerical errors in estimating the center of the interferer and slope, shoot up to give an error of 4% at maximum while estimating the shift.

# 6

# SEPARATION AND MITIGATION

Most of the existing automotive radar interference mitigation techniques rely on detecting or identifying interference before mitigating it. Post detection, interference could be avoided by moving into another frequency band where interference is not present[23], but there might be another interferer in that band. Hence many existing techniques look into mitigating interference either by reconstruction of these detected interfering samples or by nulling these samples.

The knowledge of interferer is very essential to mitigate and reconstruct the desired signal. Since a CW or FMCW interference would have a time varying frequency component post down conversion of received signal, A Short Time Fourier Transform(STFT) of the received signal would reveal most of the information regarding the interference in FMCW radar[28].

Up until now, we have discussed about ways to detect, identify and possibly mitigate interference. But we relied on the methods to estimate number of samples that are being interfered and predict slope of interference before trying to mitigate interference.

Most of the signals carry overwhelming amounts of data out of which finding the relevant information is very hard to find. Processing can be much simpler and also faster in sparse representation where few coefficients reveal the relevant information we are looking for.

In this section,we look at a novel technique to mitigate interference without actually detecting or identifying interference by compressed sensing techniques(or sparse sampling).

Use of compressed sensing techniques for mitigation [29] and separation of interference [30] for radars without any detection or identification are proposed in literature.

We propose a novel time domain solution for the interference problem by interference separation and signal reconstruction using dual basis pursuit. We show that we can mitigate interference *blindly* without any detection or identification.

## 6.1. SPARSE REPRESENTATIONS

Sparse signal representation are used for signal separation problems in[31]. This use of sparsity of signal separation is called morphological component analysis(MCA) [32]explains further about the composition of a signal separation problem.

For our case, we have considered in equation (3.13) that the mixer output has two distinctive components, one of the beat signal and the other of interference. The challenge involved in the signal separation problem of this kind is to find the domains in which the given signals are sparse.

We have proved that if the interference is wide-band post down conversion, Fig 3.10 the Power Spectral Density(PSD) of interference is uniformly distributed over the spectrum. Also we have proved in previous sections that this down converted interference would have a time dependent frequency component. So we have to realize a domain in which interference is sparse so that we can exploit the afore mentioned properties to full extent and separate the beat and interference signals.

### 6.1.1. SPARSE REPRESENTATION IN DISCRETE FOURIER TRANSFORM

In this section, we look at the sparsity of received signal. For this case, we first look into the case when we have a single object, i.e from (1.9) the received signal is a combination of a sine wave and interference.

Let us look into the DFT of received signal $s_m$, from (3.19) When we take a DFT of this signal, the coefficients are given as

$$c_1(\omega) = \sum_0^{N-1} s_m e^{-j\omega n} \tag{6.1}$$
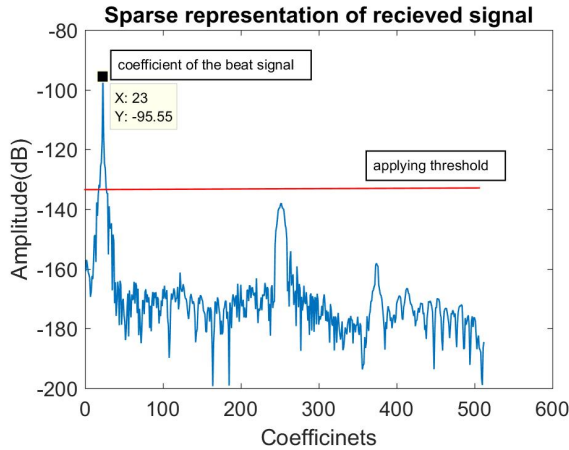


Figure 6.1: Coefficients of received signal in Fourier transform

In Fig 6.1, Coefficient of the beat signal would show up as a single peak along with the multi path coefficients of the object. The coefficients of interference are spread over all

the frequency. So if we apply a threshold over these coefficients obtained after DFT, we would only be having the coefficients of beat signal.

### 6.1.2. SPARSE REPRESENTATION IN SHORT TIME FOURIER TRANSFORM

Now let us look at Short time fourier transform for this received signal. A Short Time Fourier Transform is a windowed fourier transform. The discrete STFT is defined as

$$c_2(n,\omega) = \sum_{m=-\infty}^{\infty} s_m[m] W[n-m] e^{-j\omega n} \tag{6.2}$$

So this means, we are taking a window $W$ of n samples over the signal of a length m and taking a fourier transform for each window separately.

The window size to be used will impact the output of the STFT, we have to choose a window size such that we can track the frequency changes. These windows have to be perfect reconstruction windows to preserve the energy in the transform domain. For our case, we have used a Cosine Window for the windowing function. The coefficients of the interferer in STFT are shown in Fig 6.2.
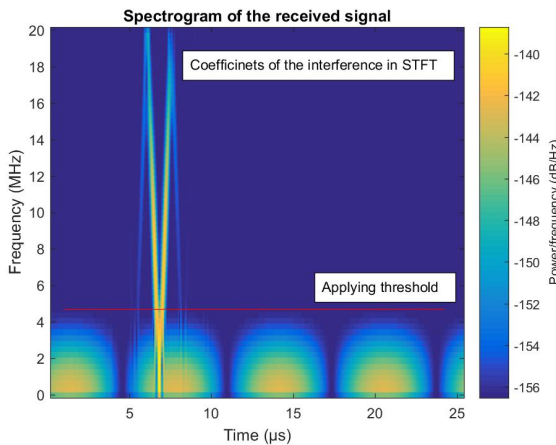


Figure 6.2: Coefficients of received signal in short time Fourier transform

### 6.1.3. SPARSE SIGNAL RESTORATION

In this section, we describe the approach restoration of signals using sparsity. This approach has gained popularity in the fields of signal processing especially for super resolution and de-noising in radar applications. Let us consider our down converted received reflected signal with no noise to be a form of

$$y = Ac, \tag{6.3}$$

where, $y$ is the received reflected signal ($s_m$), $A$ is an arbitrary transform matrix and $c$ consists of the coefficients. The estimation of $c$ from $y$ is a linear inverse problem. The standard approach to solve this problem is to choose a cost function $J(c)$ and trying to

find the coefficient $c$ that minimizes $J(c)$. Generally this cost function is chosen to be

$$J(c) = D(y - Ac) + \lambda R(c) \tag{6.4}$$

where $D(y - Ac)$ measures the discrepancy of between $y$ and $c$ and $R(c)$ is a regularization term (penalty function), details about the different penalty functions are given in [33]. The parameter $\lambda$ is a regularization parameter used to adjust the trade off between the terms.

To find the coefficient $c$ for which $Ac$ is the closest to $y$, we will use a mean square error for $D(y - Ac)$,

$$D(y - Ac) = ||y - Ac||_2^2 \tag{6.5}$$

minimizing (6.5), we get the coefficient $c$ that is the most consistent with $y$ according to the mean square criterion. But as we have seen in Fig 6.1 and Fig 6.2, both the considered transformation matrices are ill-conditioned for the respective domains. By using sparse representations, we could be able to reduce this number of unwanted coefficients and reconstruct the signal. This is exactly the role of the regularization term $R(c)$. The regularizer is used to penalize the unwanted coefficients in $y$, it is often chosen to be a $l_1$ norm [34].

### 6.1.4. SOFT THRESHOLD

For a special case of $A = I$, the cost function can be given as

$$J(c) = ||y - c||_2^2 + \lambda ||c||_1 \tag{6.6}$$

The minimizer for this equation as shown in [34] is given as,

$$y = c + \frac{\lambda}{2} sign(c) \tag{6.7}$$

where $sign(c)$ is the sign function of c. The minimizer is of the cost function is found by applying the soft threshold rule to y which is having a threshold $\lambda/2$. The soft thresholding rule can be compactly given as

$$soft(c, T) = sign(c)\max(0, |c| - T) \tag{6.8}$$

for threshold $T$. Hence the minimization of the cost function in terms of soft threshold is given as

$$c = soft(y, \lambda/2) \tag{6.9}$$

A simple soft threshold rule can be explained from Fig 6.3.
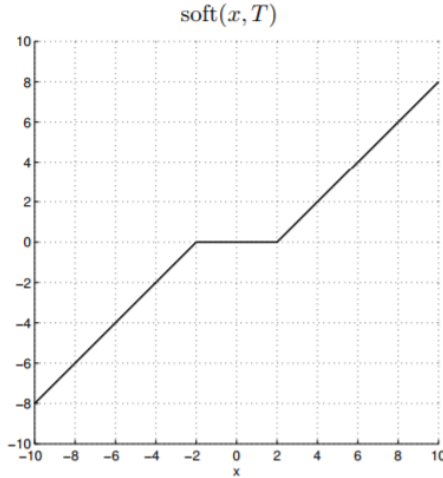
Figure 6.3: Soft threshold with T=2 [34]

For our signal separation problem, we have to make sure that we have two specific domains in which beat signal and interference are sparse respectively. After choosing these domains, we have to minimize the cost function and find the sparsest coefficients in these domains. If we reconstruct the signals with these sparse coefficients, it is intuitively clear that we might separate the interference from the beat signal and vice versa.

## 6.2. TRADITIONAL SPARSE MODELING AND REGULARIZATION

In general after finding these coefficients for the domains in which the beat signal and interference are dominant, we can reconstruct these signals as such by a simple minimization problem for signal recovery as

$$s_{mr,mi} = \underset{c_1,c_2}{\operatorname{argmin}} ||c_1||_0 + ||c_2||_0 \qquad \text{subject to} \qquad c_{1,2} \in F(s_m) \qquad (6.10)$$

where, $F$ is the inverse of the transform giving the dominant coefficients for beat signal $c_1$ and interference $c_2$ from the mixer signal $s_m$. While it is possible to analyze (6.10) under necessary assumptions, it is not particularly feasible to use $||.||_0$ as it is non-convex and is NP-hard which is not easy to solve. Because of this reason, we replace $||.||_0$ with its convex approximation $||.||_1$ , this gives us

$$s_{mr,mi} = \underset{c_1,c_2}{\operatorname{argmin}} ||c_1||_1 + ||c_2||_1 \qquad \text{subject to} \qquad c_{1,2} \in F(s_m) \qquad (6.11)$$

It might not be immediately clear that both the equations (6.10), (6.11) would give the same result, but it is also intuitive that $l_1$ norm promotes sparsity. It was shown in[35] that an arbitrary signal which is band limited in the presence of a short disturbance can be recovered completely by using $l_1$ norm. From the point of view of data modeling, we can consider sparsity as a form of *regularization*, which restricts or controls the set of

coefficients which produce the estimate of the data. Which means that *"Few non-zero coefficients should be enough to represent the data well"* [36].

## 6.3. SIGNAL SEPARATION ALGORITHM FOR AUTOMOTIVE RADAR

This section deals with the necessary information to develop an approach for automotive radar interference mitigation. We could straight away mitigate wide band interference, but it also interesting to look at the interference and its behavior in different domains. So we use signal separation methods to separate the interference and received beat signal. To separate the beat signal from the interference, we apply dual basis pursuit for signal separation. For signal separation using dual basis pursuit, we need to first know the domains in which the beat and interference are sparse.

Beat signal being a sinusoid, will have only two coefficients after taking a DFT of the signal. Interference on the other hand is a chirp signal post down conversion.

For solving the signal separation problem, let us write the observed signal $s_m$ in terms of two components from (3.13) we consider the two components to be $x_1$ and $x_2$

so

$$s_m = x_1 + x_2 \tag{6.12}$$

**6**

where $x_1$ is the beat signal component and $x_2$ is the interference component.

The morphological component analysis (MCA) approach assumes the two components of the received signal(beat and interference) are sparse in different domains[37]. A particular formulation of MCA aims to find the coefficients $c$ with respect to the transforms $A$.

$x_1$ and $x_2$ are yet to be determined, initially we have to describe each of these components using two distinct transforms $A_1$ and $A_2$ which will give sparse representations of reflected signal and interference in their own domain such that

$$x_1 = A_1 c_1, \ x_2 = A_2 c_2; \tag{6.13}$$

We have considered the beat signal to be sparse in DFT domain and interference signal to be sparse in STFT domain so the transforms $A_1$ is a Discrete Fourier Transform and $A_2$ is a Short Time Fourier Transform. The solution and sparsity of these respective transforms are given in the following section.

So, the dual basis pursuit problem is given as

$$\underset{c_1,c_2}{\operatorname{argmin}}(\lambda_1||c_1||_1 + \lambda_2||c_2||_1) \tag{6.14}$$

such that

$$s_m = A_1 c_1 + A_2 c_2; \tag{6.15}$$

For solving this optimization problem, we use SALSA[38] which is based on Alternating

Direction method of multipliers(ADMM)[39].

---

**Algorithm 4:** Signal Separation algorithm for automotive radar

---

Input : y

Initialize: $A_1$ = DFT , $A_2$= STFT, $d_i \geq 0$ for $i = 1,2$

1. $v_1 \leftarrow$ soft$(c_1 + d_1, \frac{\lambda_1}{2\mu}) - d_1$ {Find the sparsest coefficients for beat signal}

2. $v_2 \leftarrow$ soft$(c_2 + d_2, \frac{\lambda_2}{2\mu}) - d_2$ {Find the sparsest coefficients for interference}

3. $a \leftarrow y - A_1 c_1 - A_2 c_2$ {Find the residual}

4. $d_i \leftarrow \frac{1}{2} A_i^H a$ {Find the coefficient from the residual}

5. $c \leftarrow d_i + v_i$ {update the coefficient estimate}

---

## 6.4. DERIVATION OF ALGORITHM

The $N$ is the number of samples for the beat signal (3.19), $N$ is restricted to 1024.
This derivation of algorithm is given in [29], over here we revisit the algorithm for our scenario and present the results. The transforms are denoted as $A_1$ and $A_2$ where in our scenario,$A_1$ is Discrete Fourier Transform and $A_2$ is a Short Time Fourier Transform. Let us consider the constraint minimization problem,

$$\underset{c_1,c_2}{\operatorname{argmin}}(\lambda_1 C_1(c_1) + \lambda_2 C_2(c_2)) \tag{6.16}$$

such that

$$s_m = A_1 c_1 + A_2 c_2; \tag{6.17}$$

Where $C_1$ and $C_2$ are convex functions. For solving this optimization problem, we use SALSA[38] which is based on Alternating Direction method of multipliers(ADMM)[39] The first step in SALSA is to apply variable splitting by using a variable u.

$$\underset{c_1,c_2,u_1,u_2}{\operatorname{argmin}}(\lambda_1 C_1(u_1) + \lambda_2 C_2(u_2)) \tag{6.18a}$$

such that

$$s_m = A_1 c_1 + A_2 c_2; \tag{6.18b}$$

$$u_1 - c_1 = 0; \tag{6.18c}$$

$$u_2 - c_2 = 0; \tag{6.18d}$$

This optimization problem (6.18a) is to be solved iteratively by applying the ADMM method. this is given as follows

Initialize: $\mu>0$ ,$d_i$, i =1,2

Repeat,

$$c_i, u_i \leftarrow \begin{cases} \text{argmin}_{c_i, u_i} \lambda_1 C_1(u_1) + \lambda_2 C_2(u_2) & +\mu_1 ||u_1 - c_1 - \boldsymbol{d_1}||_2^2 + \mu_2 ||u_2 - c_2 - \boldsymbol{d_2}||_2^2 \\ \text{such that}: s_m = \boldsymbol{A_1} c_1 + \boldsymbol{A_2} c_2; \end{cases}$$

$$(6.19)$$

$$\boldsymbol{d_i} \leftarrow \boldsymbol{d_i} - (u_i - c_i) \tag{6.20}$$

Until convergence.

The vector $d$ is to be initialed prior to the iteration step and $\mu_i$ must be user selected values. Selection of $\mu$ does not affect the solution to which the algorithm converges, but it does affect the convergence rate.

Now, minimizing $c$ and $u$ alternatively, we obtain

$$\underset{u_1, u_2}{\text{argmin}} \leftarrow \lambda_1 C_1(u_1) + \lambda_2 C_2(u_2) + \mu_1 ||u_1 - c_1 - \boldsymbol{d_1}||_2^2 + \mu_2 ||u_2 - c_2 - \boldsymbol{d_2}||_2^2 \tag{6.21a}$$

$$c_1, c_2 \leftarrow \begin{cases} \mu_1 ||u_1 - c_1 - \boldsymbol{d_1}||_2^2 + \mu_2 ||u_2 - c_2 - \boldsymbol{d_2}||_2^2 \\ \text{such that}: s_m = \boldsymbol{A_1} c_1 + \boldsymbol{A_2} c_2; \end{cases} \tag{6.21b}$$

$$\boldsymbol{d_i} \leftarrow \boldsymbol{d_i} - (u_i - c_i) \tag{6.21c}$$

Until convergence.

$u_1$ and $u_2$ can be decoupled in (6.21), this can be written as

$$u_i \leftarrow \underset{u_i}{\text{argmin}} \lambda_i C_i(u_i) + \mu_i ||u_i - a_i \boldsymbol{d_i}||_2^2 \tag{6.22}$$

such that

$$s_m = \boldsymbol{A_1} c_1 + \boldsymbol{A_2} c_2; \tag{6.23}$$

can be given explicitly as

$$c_i = (u_i - \boldsymbol{d_i}) + \frac{1}{\mu_i} \left( \frac{1}{\mu_1} + \frac{1}{\mu_2} \right)^{-1} \times A_i^H (y - \boldsymbol{A_1}(u_1 - \boldsymbol{d_1}) - \boldsymbol{A_2}(u_2 - \boldsymbol{d_2})) \tag{6.24}$$

Since $\mu_i$ is independent of the solution, it is better to set $\mu_1 = \mu_2 = \mu$. The iterative algorithm can be written as

Initialize $\mu \geq, \boldsymbol{d_i}, i = 1, 2$ Repeat over

$$u_i \leftarrow \underset{u_i}{\text{argmin}} \lambda_i C_i(u_i) + \mu_i ||u_i - a_i \boldsymbol{d_i}||_2^2 \tag{6.25a}$$

$$a \leftarrow y - \boldsymbol{A_1}(u_1 - \boldsymbol{d_1}) - \boldsymbol{A_2}(u_2 - \boldsymbol{d_2}) \tag{6.25b}$$

$$c_i \leftarrow (u_i - \boldsymbol{d_i}) + \frac{1}{2} A_i^H(a) \tag{6.25c}$$

$$d_i \leftarrow d_i - (u_i - c_i) \tag{6.25d}$$

Until convergence
Further simplification can be made by assuming $v_i = u_i - d_i$ giving the following result
Initialize $\mu \geq, d_i, i = 1, 2$ Repeat over

$$v_i \leftarrow (\operatorname*{argmin}_{u_i} \lambda_i C_i(v_i + d_i) + \mu ||v_i - a_i||_2^2) - d_i \tag{6.26a}$$

$$a \leftarrow y - A_1(v_1) - A_2(v_2) \tag{6.26b}$$

$$a_i \leftarrow v_i + \frac{1}{2} A_i^H a \tag{6.26c}$$

$$d_i \leftarrow a_i - v_i \tag{6.26d}$$

Until convergence
to eliminate the redundant components we rearrange the terms $a_i$ and $d_i$ as
Initialize $\mu \geq, d_i, i = 1, 2$ Repeat over

$$v_i \leftarrow (\operatorname*{argmin}_{u_i} \lambda_i C_i(v_i + d_i) + \mu ||v_i - a_i||_2^2) - d_i \tag{6.27a}$$

$$a \leftarrow y - A_1(v_1) - A_2(v_2) \tag{6.27b}$$

$$d_i \leftarrow \frac{1}{2} A_i^H a a_i \leftarrow d_i + v_i \tag{6.27c}$$

Until convergence
In (6.14), we have proposed to use a DFT and STFT for enforcing sparsity for beat signal and interference respectively, with the conditions

$$A_1 = DFT \tag{6.28a}$$

$$A_2 = STFT \tag{6.28b}$$

$$C_1(c_1) = ||c_1||_1 \tag{6.28c}$$

$$C_2(c_2) = ||c_2||_1 \tag{6.28d}$$

Here, we have used function C for enhancing sparsity of the input signal ($l_1$ norm in this case). $\mu$ and $\lambda$ are user specified.
The solution to minimization problem, in (6.27) can be expressed explicitly by soft thresholding.
The minimization of $v_i$ $\gamma ||v||_1 + ||v - y||_2^2$ is given as $v_i = soft(\mathbf{y}, \gamma/2)$ is called the soft thresholding rule $soft(\mathbf{y}, T)$ where $T$ is the threshold applied.[40] which is defined as

$$soft(\mathbf{y}, T) = \mathbf{y} \, max(0, \frac{T}{|y|}) \qquad\qquad y \in \mathbb{C}, T \in \mathbb{R} \tag{6.29}$$

## 6.5. EXPERIMENTAL SETUP FOR INTERFERENCE MITIGATION

We have setup simulations in the presence of in terms of CW and FMCW interferers and also setup an experiment experiment with a Stepped CW interferer to demonstrate the success of proposed algorithm. A new generation NXP Dolphin transceiver chip at 78.8 GHz center frequency with a bandwidth of 1.0 GHz is set up as automotive radar. A simple pendulum is used to simulate a moving target. The pendulum, consisting of a 0 dBm$^2$ (at 77 GHz) trihedral reflector mounted on a swinging arm of 1 m length, is located at a 5 m range from the radar unit. The interference source is located at the same range with a 20 degree offset. A 78 GHz CW signal is generated using a Keysight N542A PNA with a WR-10 frequency extension module and is transmitted via a 20dB standard gain horn.

## 6.6. USING SPARSITY FOR INTERFERENCE MITIGATION

We can see that the interference can be perfectly separated (Fig 6.5) from the received signal (Fig 6.4). As a result, the integrated interference power can be reduced by 23 dB resulting in an attenuated interference floor (Fig 6.6 ) and the resultant beat signal is shown in Fig 6.7.
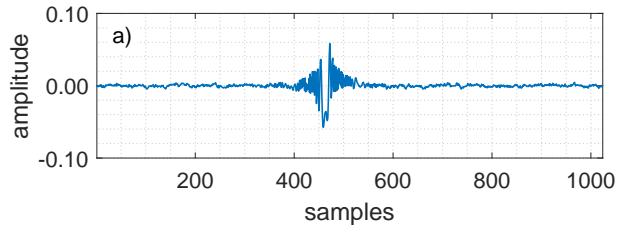


Figure 6.4: received signal
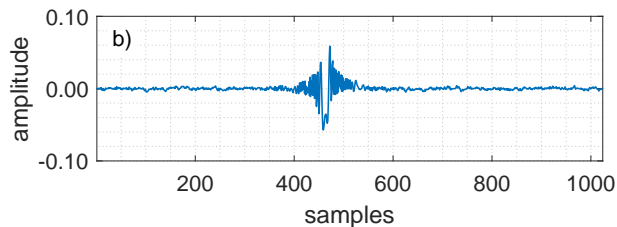


Figure 6.5: interference signal
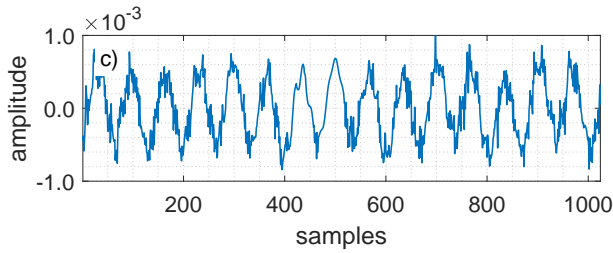
Figure 6.6: interference mitigated signal
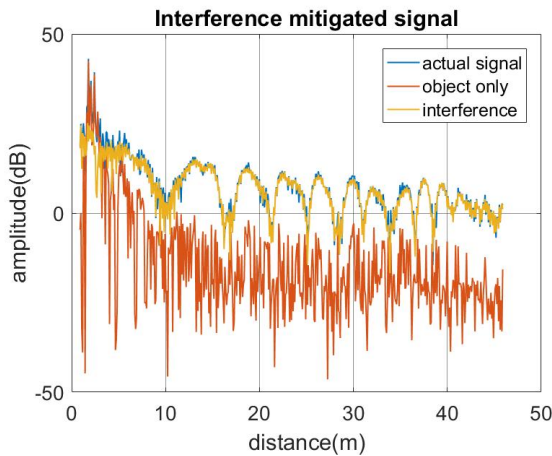


Figure 6.7: mitigation using signal separation methods

## 6.7. RESULTS AND DISCUSSION

To demonstrate this algorithm, we have collected data where interference and object co-exist in range-doppler domain. Fig 6.8a shows the range-doppler map of a particular snapshot of the collected data in the presence of interference and Fig 6.8b is the collected data post application of ground clutter filter. The interference mitigated signal is shown in Fig 6.9a along with the separated interference in Fig 6.9b. Hence, with the proposed algorithm we separate the interference and mitigate the interference from the received signal component.

(a) Collected signal with target, interference and ground clutter

(b) collected signal after ground clutter filter
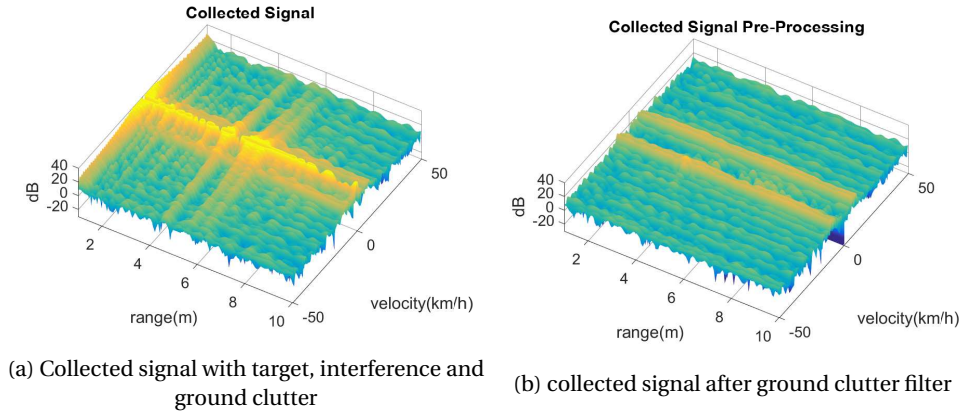
Figure 6.8: Collected signal before and after ground clutter filter



(a) Target after application of separation algorithm

(b) Separated interference signal
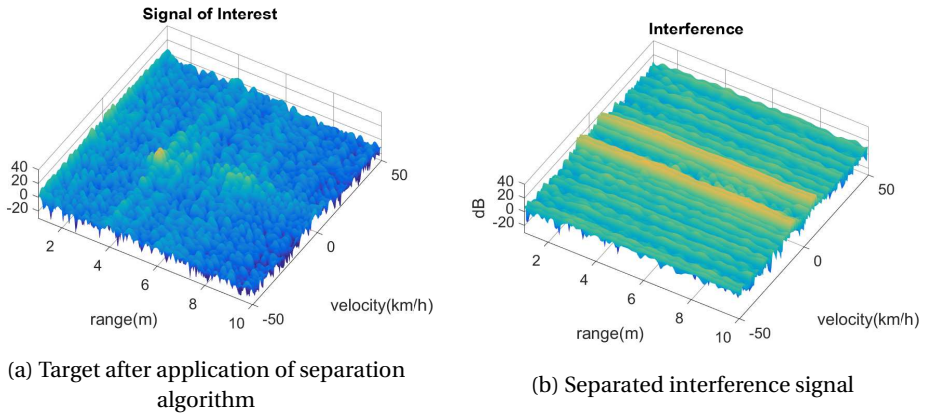
Figure 6.9: Signal and interference post separation

This algorithm is shown to work even for a worst case scenario when the object is buried under the interference floor.

## 6.8. CONCLUSIONS

With this method, we can mitigate the interference blindly just by knowing the domains in which the interference and beat signal are sparse. We have shown that the beat signal is sparse in DFT as shown in Fig 6.1 and interference is sparse in STFT as shown in Fig 6.2. With this information, we have shown that the interference can be separated as shown in Fig 6.5 and the interference mitigated beat signal as shown in Fig 6.4 and have seen that about 23 dB of integrated interference power removed.

Also for the collected data, with the application of ground clutter filter, the algorithm works better as shown in Fig 6.8. We also have shown the separated beat and interference

signal in Fig 6.9. In these figures we have seen that the target which is buried under the interference can also be separated with this algorithm. Adaptive parameter application might enhance the performance of this algorithm, this topic is under active research and requires further investigation.

**6**

# 7

# CONCLUSIONS AND FUTURE IMPLEMENTATIONS

The goal of this thesis was to investigate FMCW system interference and propose methods to detect, identify, mitigate/avoid and separate interference for various interference scenarios. With an introduction to radar and its uses in automotive, we described at the most prevalent FMCW radar system for automotive and also briefly looked in PMCW system. To understand interference and how it is unfolded at every stage of the block diagram, we have set up a simulation chain in MATLAB for FMCW system with three different interference scenarios namely, FMCW interference, CW interference and PMCW interference. We described in detail how the interference looks like on every block and proved them with necessary equations in Chapter 3. With this information obtained, we have realized that down converted interference would possess wide band properties.

With this information given, in Chapter 4 we proposed a method to detect interference post down conversion using a HPF with a cut off specifically derived from the beat signal. This cut off frequency corresponds to the distance at which the object power level would be below the noise floor. It was shown that with proper design of HPF cut off, we can attenuate the beat signal as well as isolate the interference for detection and derived the cut off frequency of HPF to be at 6MHz. The maximum number of interference samples that we can detect in the presence of HPF is derived in equation (4.27). With this method, we were able to detect interference even if the interferer peak power is less than the reflected signal power. We compare the performance of this detector in detecting a single sample and multiple samples and realized that there is a loss of about 3dB while detecting multiple samples. We also described that compound filtering impacts the performance of our detector by 0.6dB. The results of the detection algorithm for detecting the interference with the given transmitted power and a probability of 0.8 is given as follows

For detecting a single sample,

| interferer | probability | min.INR(dB) |
|:----------:|:-----------:|:-----------:|
| FMCW | 0.8 | 13 |
| CW | 0.8 | 12 |

For detecting 10 samples,

| interferer | probability | min.INR(dB) | % of the interferer detected |
|:----------:|:-----------:|:-----------:|:----------------------------:|
| FMCW | 0.8 | 16 | 30 |
| CW | 0.8 | 14 | 20 |

With these results we can conclude that we need at least 12 dB of INR to detect a single sample of CW interferer with a probability of 0.8 where as FMCW interferer would need at least 13 dB of INR to be detected.

Similarly, to detect 10 samples, with a probability of 0.8, we need at least 14 dB for CW interferer and at least 16 dB for FMCW interferer.

In Chapter 5, we investigated how this information on the interfering samples can be used in estimating the slopes by using equations (5.8),(5.9) and center of the interference using equation (5.11). With accruing as much information as possible from the interference, we have predicted the bandwidth of the interferer. To avoid the interference completely, we suggested an algorithm to shift the center frequency of transmission. This algorithm is demonstrated in the presence of FMCW and CW interference along with the results in section 5.3. We have seen that the interference can be completely avoided by using this algorithm.

| type | interferer | actual shift(MHz) | estimated shift(MHz) |
|:----:|:----------:|:-----------------:|:--------------------:|
| sawtooth | FMCW | 500 | 520 |
| triangular | FMCW | 300 | 310 |

| interferer | actual center frequency(MHz) | estimated center frequency(MHz) |
|:----------:|:----------------------------:|:-------------------------------:|
| CW | 100 | 104 |

The numerical errors in estimating the center of the interferer and slope shoots up to give an error of 4% at maximum while estimating the shift.

Finally in Chapter 6, we have proposed a novel technique to mitigate the interference *blindly* by using Compressed sensing techniques and have investigated the SINR improvement that can be achieved by using this algorithm. Applying it to the real data we have seen a reduction in integrated interference floor of about 23 dB as shown in Fig 6.7. Also, as a worst case scenario, we have seen that the object which is under the interference floor can also be detected with our algorithm as shown in Fig 6.5 and Fig 6.6.

## 7.1. FUTURE IMPLEMENTATIONS

- We have looked into the interference post down conversion and concluded that the interference will posses wide band properties. Also by using Fresnel integrals we have seen how the interference will unfold in lower and higher interference times. The PSD of the interferer has not been estimated in our thesis. If we are able to predict this interference PSD post down conversion of the interferer as

such, interference can be completely reconstructed in spectral domain and a simple subtraction in spectral domain might give a high SINR ratio. This approach is suggested for further research.

- Most of the equations derived and used in this thesis are based on the fact that interference has an instantaneous frequency which is linearly dependent on time. PMCW interferer on the other hand has properties similar to noise as well. Mitigating PMCW interferer for an FMCW system is still an open question.

- Most of the existing mitigation techniques as well as this thesis focuses a single interferer system. The most convenient way is to avoid multiple interferers is by hopping into another frequency band because reconstructing the time domain signal might be a difficult task in presence of multiple interfering systems. Although, mitigation in presence of multiple interfering systems is suggested for further research.

**7**

## REFERENCES

[1] G. M. Brooker, "Mutual interference of millimeter-wave radar systems," *IEEE Transactions on Electromagnetic Compatibility*, vol. 49, pp. 170–181, Feb 2007.

[2] M. Goppelt, H. L. Blocher, and W. Menzel, "Analytical investigation of mutual interference between automotive fmcw radar sensors," in *2011 German Microwave Conference*, pp. 1–4, March 2011.

[3] M. Goppelt, H. Blocher, and W. Menzel, "Automotive radar, investigation of mutual interference mechanisms," *Advanced Radio Sciences*, 2010.

[4] T. Schipper, T. Mahler, M. Harter, L. Reichardt, and T. Zwick, "An estimation of the operating range for frequency modulated radars in the presence of interference," in *2013 European Radar Conference*, pp. 227–230, Oct 2013.

[5] A. G. Stove, "Modern fmcw radar - techniques and applications," in *First European Radar Conference, 2004. EURAD.*, pp. 149–152, Oct 2004.

[6] N. Levanon and B. Getz, "Comparison between linear fm and phase-coded cw radars," *IEE Proceedings - Radar, Sonar and Navigation*, vol. 141, pp. 230–240, Aug 1994.

[7] M. A. Richards, J. A. Scheer, and W. A. Holm, *Principles of Modern Radar: Basic Principles*. Institution of Engineering and Technology, 2010.

[8] J. O. Smith, *Mathematics of the Discrete Fourier Transform (DFT)*. http://ccrma.stanford.edu/~jos/mdft/, accessed (date accessed). online book, 2007 edition.

[9] M. Kunert, "The eu project mosarim: A general overview of project objectives and conducted work," in *2012 9th European Radar Conference*, pp. 1–5, Oct 2012.

[10] M. Sriram, B. Sachin, R. Karthik, S. Karthik, R. Sandeep, and G. B. Paul, "Interference detection in a frequency modulated continuous wave (fmcw) radar system," 2016.

[11] W. Yuu and N. Kazuma, "Interference determination method and fmcw radar using the same," 2007.

[12] N. Kazuma and W. Yuu, "Fmcw radar device and method for detecting interference," 2006.

[13] C. B. Lae, S. S. Gu, L. J. Soo, and L. J. Min, "Method for suppression and detection of the interference signal in frequency modulated continuous wave radars and storage medium thereof," 2013.

[14] S. Mai, "Interference determination method and fmcw radar," 2008.

[15] T. Schipper, M. Harter, L. Zwirello, T. Mahler, and T. Zwick, "Systematic approach to investigate and counteract interference-effects in automotive radars," in *2012 9th European Radar Conference*, pp. 190–193, Oct 2012.

[16] B. E. Tullsson, "Topics in fmcw radar disturbance suppression," in *Radar 97 (Conf. Publ. No. 449)*, pp. 1–5, Oct 1997.

[17] J. Bechter and C. Waldschmidt, "Automotive radar interference mitigation by reconstruction and cancellation of interference component," in *2015 IEEE MTT-S International Conference on Microwaves for Intelligent Mobility (ICMIM)*, pp. 1–4, April 2015.

[18] H. C.Fischer, M.Gopplet and J.Dickmann, "Minimizing interference in automotive radar using digital beamforming," *Adv. Radio Sci.*, 2011.

[19] J. Bechter, K. Eid, F. Roos, and C. Waldschmidt, "Digital beamforming to mitigate automotive radar interference," in *2016 IEEE MTT-S International Conference on Microwaves for Intelligent Mobility (ICMIM)*, pp. 1–4, May 2016.

[20] Z. Jian-Hui, L. Guo-Sui, G. Hong, and S. Wei-Min, "A novel transmit signal based on high range-resolution concept for flar or aicc system applications," in *2001 CIE International Conference on Radar Proceedings (Cat No.01TH8559)*, pp. 81–84, 2001.

[21] M. Barjenbruch, D. Kellner, K. Dietmayer, J. Klappstein, and J. Dickmann, "A method for interference cancellation in automotive radar," in *2015 IEEE MTT-S International Conference on Microwaves for Intelligent Mobility (ICMIM)*, pp. 1–4, April 2015.

[22] J. Matas, O. Chum, M. Urban, and T. Pajdla, "Robust wide-baseline stereo from maximally stable extremal regions," *Image and Vision Computing*, vol. 22, no. 10, pp. 761 – 767, 2004. British Machine Vision Computing 2002.

[23] J. Bechter, C. Sippel, and C. Waldschmidt, "Bats-inspired frequency hopping for mitigation of interference between automotive radars," in *2016 IEEE MTT-S International Conference on Microwaves for Intelligent Mobility (ICMIM)*, pp. 1–4, May 2016.

[24] T. K. Idnin PASYA, Hiroshi KATO, "Interference suppression performance of automotive uwb radars using pseudo random sequences," in *RADIOENGINEERING, VOL. 24, NO. 4*, 2015.

[25] J. R. Klauder, A. C. Price, S. Darlington, and W. J. Albersheim, "The theory and design of chirp radars," *The Bell System Technical Journal*, vol. 39, pp. 745–808, July 1960.

[26] M. A.Richards, *Fundamentals of radar signal processing*. McGraw Hill Professional, 2005.

[27] J. Bechter, K. D. Biswas, and C. Waldschmidt, "Estimation and cancellation of interferences in automotive radar signals," in *2017 18th International Radar Symposium (IRS)*, pp. 1–10, June 2017.

[28] S. Tullsson, Bert-eric (Järfalla, "Procedure for the elimination of interference in a radar unit of the fmcw type," October 2002.

[29] F. Uysal, I. Selesnick, and B. M. Isom, "Mitigation of wind turbine clutter for weather radar by signal separation," *IEEE Transactions on Geoscience and Remote Sensing*, vol. 54, pp. 2925–2934, May 2016.

[30] L. H. Nguyen and T. D. Tran, "Interference separation for uwb radar signals from entropy-driven robust pca," in *2017 IEEE Radar Conference (RadarConf)*, pp. 0389–0393, May 2017.

[31] J.-F. Aujol, G. Aubert, L. Blanc-Féraud, and A. Chambolle, "Image decomposition into a bounded variation component and an oscillating component," *Journal of Mathematical Imaging and Vision*, vol. 22, pp. 71–88, Jan 2005.

[32] I. Selesnick, *Introduction to Sparsity in Signal Processing*. Conexxtions,2012.

[33] I. Selesnick, "Penalty and shrinkage functions for sparse signal processing."

[34] I. W. SELESNICK, "Sparse signal restoration," Connexions, 2009.

[35] D. L. Donoho and B. F. Logan, "Signal recovery and the large sieve," *SIAM Journal on Applied Mathematics*, vol. 52, no. 2, pp. 577–591, 1992.

[36] Y. C. Eldar, *Compressed Sensing: Theory and Applications.* Cambridge University Press, 2012.

[37] J.-L. Starck, Y. Moudden, J. Bobina, M. Elad, and D. Donoho, "Morphological component analysis," *Proc. SPIE Wavelets XI,vol. 5914, pp. 9–19*, 2005.

[38] M. V. Afonso, J. M. Bioucas-Dias, and M. A. T. Figueiredo, "Fast image recovery using variable splitting and constrained optimization," *IEEE Transactions on Image Processing*, vol. 19, pp. 2345–2356, Sept 2010.

[39] S. Boyd, N. Parikh, E. Chu, B. Peleato, and J. Eckstein, "Distributed optimization and statistical learning via the alternating direction method of multipliers," *Found. Trends Mach. Learn.*, 2011.

[40] M. J. Fadili, J. L. Starck, J. Bobin, and Y. Moudden, "Image decomposition and separation using sparse representations: An overview," *Proceedings of the IEEE*, vol. 98, pp. 983–994, June 2010.